

Bayes Risk for Goodness of Fit Tests

Nicholas G. Polson², Vadim Sokolov³, and Daniel Zantedeschi⁴

²Booth School of Business, University of Chicago, Chicago, IL 60637, ngp@chicagobooth.edu

³Volgenau School of Engineering, George Mason University, Fairfax, VA 22030, vsokolov@gmu.edu

⁴School of Information Systems, Muma College of Business, University of South Florida, Tampa, FL 33620, danielz@usf.edu

February 2026

Abstract

We develop a unified framework for goodness-of-fit (GOF) testing through the lens of Bayes risk. Classical GOF procedures are commonly calibrated either at fixed significance level (CLT scale) or through exponential error exponents (LDP scale). We establish that Bayes-risk optimal calibration operates on the moderate-deviation (MDP) scale, producing canonical $\sqrt{\log n}$ inflation of rejection thresholds and polynomially decaying Type I error.

Our main contributions are: (i) we formalise the Rubin–Sethuraman program for KS-type statistics as a risk-calibration theorem with explicit regularity conditions on priors and empirical-process functionals; (ii) we develop the precise connection between Bayes-risk expansions and Sanov information asymptotics, showing how $\log n$ -order truncations arise naturally when risk, rather than pure exponents, is the evaluation criterion; (iii) we provide detailed applications to location testing under Laplace families, shape testing via Bayes factors, and connections to Fisher information geometry. The organizing principle throughout is that sample size enters Bayes-optimal GOF cutoffs through the MDP scale, unifying KS-based and Sanov-based perspectives under a single risk criterion.

Keywords: Bayes risk; goodness-of-fit; moderate deviations; Kolmogorov–Smirnov; Sanov theorem; Bayes factors; Fisher information.

1 Introduction

Goodness-of-fit (GOF) testing occupies a central position in statistical methodology, serving as the primary mechanism for model criticism, specification search, and validation of probabilistic assumptions. Classical GOF procedures, including Kolmogorov–Smirnov (KS) statistics, likelihood-ratio tests, chi-squared tests, and entropy-based criteria, have been studied extensively under two dominant asymptotic frameworks: *fixed- α calibration* (CLT scale), where critical values control Type I error at a constant level, and *exponential error exponents* (LDP scale), where performance is characterised by large-deviation rate functions and Chernoff bounds (Chernoff, 1952; Dembo and Zeitouni, 1998).

Neither framework is appropriate when the inferential objective is *Bayes risk minimisation* (cf. Berger, 1985; Le Cam, 1986). Fixed- α calibration ignores the fact that, as sample size grows, an increasing number of alternatives become statistically distinguishable and must be jointly serviced. Pure large-deviation calibration enforces overly stringent rejection thresholds that sacrifice power against local and moderate alternatives, leading to suboptimal Bayesian risk even when Type I error is extremely small.

The central message of this paper is that Bayesian calibration of GOF tests naturally operates on the *moderate-deviation* (MDP) scale. This intermediate regime, lying strictly between CLT and LDP scales, arises because the number of alternatives that a sample of size n can distinguish from the null grows polynomially, and a Bayes-risk criterion must service all of them. Concretely, at sample size n the experiment resolves distributions at Fisher distance $\sqrt{\log n/n}$ from the null; any prior that is absolutely continuous near \mathcal{F}_0 places polynomial mass in this shell. Balancing false rejections against the cumulative missed-detection cost over this growing set of distinguishable alternatives forces thresholds to inflate as $\sqrt{\log n}$, Type I error to decay polynomially, and Bayes risk to concentrate on the boundary shell.

The information-theoretic lineage of this perspective is extensive. Sanov (1957) established that empirical measures satisfy a large-deviation principle with Kullback–Leibler rate function. Bahadur (1960) and Bahadur and Rao (1960) showed that polynomial prefactors in tail probabilities affect statistical efficiency at moderate scales. Rubin and Sethuraman (1965a,b) analysed Bayes risk for empirical-process statistics and derived moderate-deviation optimality for KS-type procedures. Good (1955) emphasised weight-of-evidence interpretations of log-likelihood ratios, while Pearson’s χ^2 test and entropy-deficit criteria (Jaynes, 1957) were later shown to share identical large-deviation rate functions. What has been missing is a *single generative mechanism* that explains why these distinct threads converge at the MDP scale, and a template (Lemma 2.8) that makes each instantiation a two-line corollary.

Our main contributions are as follows. We state an explicit *Bayes-Risk MDP Principle* (Section 2) and prove it as a theorem under regularity conditions that cover KS-type statistics, Sanov-based tests, and standard parametric GOF problems. We formalise the Rubin–Sethuraman program for KS statistics (Section 3) as a risk-calibration theorem with sharp constants, showing that the Bayes-optimal threshold satisfies $t_n^* = \sqrt{(\kappa/4) \log n} + O(\sqrt{\log \log n})$. We develop the connection between Bayes risk and Sanov information asymptotics (Section 4), showing that the effective KL exponent is truncated to $O(\log n/n)$ under Bayes-risk optimisation, and providing the information-theoretic interpretation of MDP scaling. Finally, we apply the theory to location testing under Laplace families, shape testing via Bayes factors, multinomial GOF, and Fisher information geometry (Sections 5–6). Rubin–Sethuraman identify the MDP calibration in the KS

setting; our contribution is to isolate the underlying (ρ, κ) mechanism and show it applies uniformly across GOF statistics, including empirical-process, KL/Sanov, multinomial, and parametric geometric instances.

Recent work (Datta et al., 2026) develops a unified theory of Bayesian hypothesis testing via moderate deviation asymptotics, focusing on Bayes factors and integrated risk expansions. While both approaches identify the moderate deviation regime as central for Bayesian calibration, the present paper isolates a distinct mechanism: a generic risk decomposition template based solely on (i) Gaussian-type null tails and (ii) local prior mass exponents. Our results do not depend on Bayes factors or likelihood-ratio structure per se. Instead, Theorem 2.6 and Lemma 2.8 provide a reusable calibration principle applicable to a broad class of statistics, including goodness-of-fit tests, empirical processes, and divergence-based procedures. In this sense, the moderate deviation scaling emerges here as a structural consequence of risk balancing, rather than as a property specific to Bayesian hypothesis testing. Our references to Dawid’s decomposition and prequential results follow the published accounts in Dawid (2011, 1992).

The paper is organised as follows. Section 2 formalises the GOF testing problem, defines Bayes risk, and states the organizing principle. Section 3 establishes Bayes-risk optimality of MDP calibration for KS-type statistics. Section 4 develops the Sanov/information-asymptotic perspective. Section 5 gives applications. Section 6 connects to Fisher information geometry. Section 7 provides numerical verification of the calibration template. Section 8 discusses implications and extensions. Appendix B provides a compact triangulation linking Bayes factors (Good), large deviations (Hoeffding), entropy geometry (Jaynes), and Wilks’ chi-square limit through KL curvature, clarifying the geometric foundation of the moderate-deviation boundary derived here.

2 Setup and the Bayes-Risk GOF Principle

2.1 The Testing Problem

Let X_1, \dots, X_n be i.i.d. with distribution F on a measurable space $(\mathcal{X}, \mathcal{A})$. The goodness-of-fit testing problem is

$$H_0 : F \in \mathcal{F}_0 \quad \text{vs.} \quad H_1 : F \in \mathcal{F}_1, \quad (1)$$

where \mathcal{F}_0 and \mathcal{F}_1 are disjoint classes of distributions. We allow several standard configurations: a simple null $\mathcal{F}_0 = \{F_0\}$; a parametric null $\mathcal{F}_0 = \{F_\theta : \theta \in \Theta_0\}$ (see Kiefer and Wolfowitz, 1956, for consistency under growing parameter spaces); and composite or nonparametric alternatives. A (possibly randomized) test is a measurable map $\delta_n : \mathcal{X}^n \rightarrow [0, 1]$, where $\delta_n(x^n)$ is the probability of rejecting H_0 given data x^n .

2.2 Empirical Measures and GOF Statistics

Many GOF procedures are functionals of the empirical measure

$$\hat{\pi}_n := \frac{1}{n} \sum_{i=1}^n \delta_{X_i}, \quad (2)$$

or equivalently the empirical distribution function $F_n(t) = n^{-1} \sum_{i=1}^n \mathbf{1}\{X_i \leq t\}$. GOF statistics can be written as $T_n = \mathsf{T}(\hat{\pi}_n; F_0)$ for a discrepancy functional T . Representative examples include the Kolmogorov–Smirnov statistic $S_n = \sup_t |F_n(t) - F_0(t)|$, Cramér–von Mises, Anderson–Darling, and likelihood-ratio statistics.

2.3 Bayes Risk Formulation

We embed GOF testing in Bayesian decision theory by placing priors on \mathcal{F}_0 and \mathcal{F}_1 and assigning costs to Type I and Type II errors.

Definition 2.1 (Bayes risk for testing). Let $\pi_0, \pi_1 > 0$ with $\pi_0 + \pi_1 = 1$ denote prior probabilities on the hypotheses. Let Π_0 be a probability measure on \mathcal{F}_0 and Π_1 a probability measure on \mathcal{F}_1 . Let $L_0, L_1 > 0$ denote the losses for Type I and Type II errors. The *Bayes risk* of a test δ_n is

$$B_n(\delta_n) = \pi_0 L_0 \mathbb{E}_{F \sim \Pi_0} [\mathbb{E}_F [\delta_n(X^n)]] + \pi_1 L_1 \mathbb{E}_{F \sim \Pi_1} [\mathbb{E}_F [1 - \delta_n(X^n)]] \quad (3)$$

Remark 2.2 (Error probabilities and averaged errors). For any F , define the rejection probability $\alpha_n(F) := \mathbb{E}_F [\delta_n(X^n)]$. The prior-averaged errors are $\bar{\alpha}_n := \mathbb{E}_{F \sim \Pi_0} [\alpha_n(F)]$ and $\bar{\beta}_n := \mathbb{E}_{F \sim \Pi_1} [1 - \alpha_n(F)]$, so that $B_n(\delta_n) = \pi_0 L_0 \bar{\alpha}_n + \pi_1 L_1 \bar{\beta}_n$. Bayes calibration balances Type I and Type II errors after averaging over the null and alternative classes.

2.4 Reduction to a Likelihood-Ratio Form

Define the prior predictive (mixture) measures on \mathcal{X}^n :

$$M_0^{(n)}(\cdot) := \int P_F^{\otimes n}(\cdot) \Pi_0(dF), \quad M_1^{(n)}(\cdot) := \int P_F^{\otimes n}(\cdot) \Pi_1(dF).$$

Proposition 2.3 (Bayes-optimal test). *Assume $M_0^{(n)}$ and $M_1^{(n)}$ are mutually absolutely continuous. Then any Bayes-risk minimiser can be taken to be a threshold rule in the predictive likelihood ratio $\Lambda_n(X^n) := dM_1^{(n)}/dM_0^{(n)}(X^n)$:*

$$\delta_n^*(X^n) = \mathbf{1}\{\Lambda_n(X^n) > \tau\} + \gamma \mathbf{1}\{\Lambda_n(X^n) = \tau\}, \quad \tau := \frac{\pi_0 L_0}{\pi_1 L_1}, \quad (4)$$

for some $\gamma \in [0, 1]$.

Proof. The data-then-posterior form (6) shows $B_n(\delta_n) = \int [\int L(F, \delta_n) \Pi(dF \mid x^n)] m(x^n) dx^n$. For 0–1 loss with costs L_0, L_1 , the inner integral is minimised pointwise by choosing $\delta_n(x^n) = 1$ iff $\pi_1 L_1 \mathbb{P}(F \in \mathcal{F}_1 \mid x^n) > \pi_0 L_0 \mathbb{P}(F \in \mathcal{F}_0 \mid x^n)$. By Bayes' rule, $\mathbb{P}(F \in \mathcal{F}_i \mid x^n) \propto \pi_i dM_i^{(n)}/dx^n$, so the decision reduces to $dM_1^{(n)}/dM_0^{(n)} > \pi_0 L_0 / (\pi_1 L_1)$. This is the classical Bayesian binary hypothesis testing result (Berger, 1985, Ch. 4). \square

2.5 Fubini Decompositions

A key structural device is the ability to rewrite Bayes risk by swapping the order of integration between the data space and the model space. Let $\Pi = \pi_0 \Pi_0 + \pi_1 \Pi_1$ denote the mixture prior, $p(x^n | F)$ a density version, and $m(x^n) := \int p(x^n | F) \Pi(dF)$ the marginal.

The *prior-then-data form* writes Bayes risk as an expectation of loss under the joint:

$$B_n(\delta_n) = \int_{\mathcal{F}_0 \cup \mathcal{F}_1} \int_{\mathcal{X}^n} L(F, \delta_n(x^n)) p(x^n | F) dx^n \Pi(dF). \quad (5)$$

By Fubini, the *data-then-posterior form* is:

$$B_n(\delta_n) = \int_{\mathcal{X}^n} \left[\int_{\mathcal{F}_0 \cup \mathcal{F}_1} L(F, \delta_n(x^n)) \Pi(dF | x^n) \right] m(x^n) dx^n. \quad (6)$$

Equation (5) is useful for understanding how the alternative space contributes to risk; (6) is the operational form underlying the proof of Proposition 2.3.

2.6 Three Calibration Regimes

Calibration of a GOF test amounts to choosing a rejection threshold t_n for a statistic T_n . Write $\alpha_n \asymp \mathbb{P}_{F_0}(T_n > t_n)$.

Definition 2.4 (Calibration regimes). The canonical regimes are: the *CLT regime*, where $\alpha_n = \alpha \in (0, 1)$ is fixed and $t_n = O(1)$ for standardised statistics; the *MDP regime*, where $\alpha_n = n^{-c}$ for some $c > 0$ and $t_n = O(\sqrt{\log n})$ for Gaussianised statistics; and the *LDP regime*, where $\alpha_n = \exp(-cn)$ for some $c > 0$ and $t_n = O(\sqrt{n})$ for Gaussianised statistics.

2.7 The Organizing Principle

The following principle is the structural backbone of this paper. Each main theorem instantiates it in a specific GOF setting.

Principle 2.5 (Bayes risk forces the MDP scale). Under Bayes-risk optimization for goodness-of-fit testing, the optimal rejection threshold inflates at order $\sqrt{\log n}$ for Gaussianised statistics, because risk trades Type I polynomial decay against Type II detection under prior-weighted mixtures. Specifically, whenever (i) the null tail of the GOF statistic is sub-Gaussian at the \sqrt{n} -scale, and (ii) the alternative prior Π_1 assigns polynomial mass to shrinking neighbourhoods of \mathcal{F}_0 , the Bayes-optimal threshold satisfies $t_n^* \asymp \sqrt{\log n}$ and the Type I error decays polynomially: $\alpha_n^* \asymp n^{-c}$ for a problem-dependent constant $c > 0$.

The reduction chain that this principle encodes is:

GOF problem \rightarrow Bayes risk criterion \rightarrow mixture tail / truncation
 \rightarrow MDP scaling \rightarrow canonical thresholds.

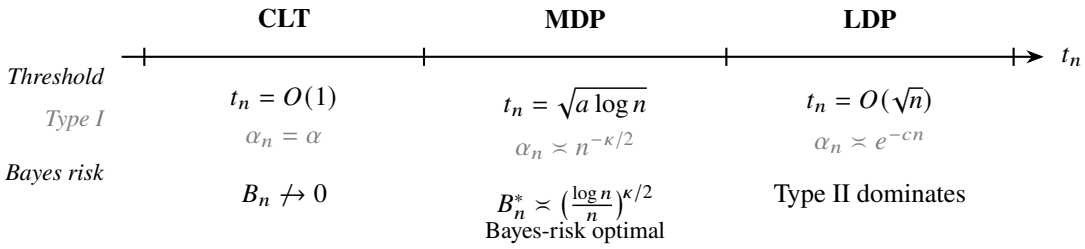


Figure 1: The three calibration regimes. Only the moderate-deviation (MDP) scale achieves vanishing Bayes risk at the optimal rate.

Each main result in this paper follows this chain: KS/empirical-process functionals (Theorem 3.6), Sanov/LDP truncation (Theorem 4.3), concrete models, namely Laplace location (Theorem 5.4) and multinomial chi-squared (Theorem 5.8), and Fisher geometry (Theorem 6.2).

2.8 First Formal Anchor

We now state the first formal version of the principle. Different GOF statistics induce different Gaussian tail constants; we normalise them as follows.

Convention (Gaussian tail normalisation). Throughout, we parameterise Gaussian-type null tails in the form

$$\mathbb{P}_{F_0}(\sqrt{n} T_n > t) \asymp \exp(-2\rho t^2), \quad t \rightarrow \infty, \quad (7)$$

where $\rho > 0$ is a statistic-specific constant. The factor 2 is purely notational; it matches the Kolmogorov tail $\sim 2e^{-2t^2}$ and could be absorbed into ρ ; we keep it to simplify later specialisations. For the KS statistic, $\rho = 1$.

Notation. Throughout, $f \asymp g$ means $c g \leq f \leq C g$ for positive constants c, C independent of n . Where a statistic-specific polylogarithmic prefactor refines the template rate (e.g., the Rubin–Sethuraman shell factor for KS), it is stated explicitly in the specialised theorem.

Theorem 2.6 (MDP is Bayes-risk optimal for GOF). *Suppose:*

- (i) **Sub-Gaussian null tail:** the GOF statistic satisfies $\mathbb{P}_{F_0}(\sqrt{n} T_n > t) \asymp \exp\{-2\rho t^2\}$ for $t \rightarrow \infty$;
- (ii) **Local detectability:** alternatives at distance ε from \mathcal{F}_0 are detected once $\varepsilon \gg t/\sqrt{n}$;
- (iii) **Polynomial prior mass:** $\Pi_1(\{F : d(F, \mathcal{F}_0) \leq \varepsilon\}) \asymp \varepsilon^\kappa$ for small $\varepsilon > 0$.

Set $t_n = \sqrt{a \log n}$. Then the Bayes risk of the threshold test δ_{n,t_n} satisfies

$$B_n(t_n) \asymp n^{-2\rho a} + (a \log n/n)^{\kappa/2}. \quad (8)$$

Minimising over a yields $a^* = \kappa/(4\rho)$, whence the Bayes-optimal threshold is $t_n^* = \sqrt{\kappa \log n/(4\rho)} + O(\sqrt{\log \log n})$. Type I error decays polynomially as $\alpha_n^* \asymp n^{-\kappa/2}$, and the optimal Bayes risk is $B_n^* \asymp (\log n/n)^{\kappa/2}$. By contrast, fixed- α calibration ($a = 0$) leaves B_n bounded away from zero, and LDP calibration ($a \propto n$) forces Type II dominance.

Proof. Decompose the Bayes risk as $B_n(t_n) = \pi_0 L_0 \alpha_n(t_n) + \pi_1 L_1 \bar{\beta}_n(t_n)$, absorbing the positive constants into \asymp .

Type I term. Setting $t_n = \sqrt{a \log n}$ in assumption (i) gives $\alpha_n \asymp \exp\{-2\rho a \log n\} = n^{-2\rho a}$.

Type II term. By assumption (ii), alternatives at distance $\varepsilon > t_n/\sqrt{n} = \sqrt{a \log n/n}$ from \mathcal{F}_0 are detected with probability tending to one; alternatives closer than this radius contribute the bulk of the missed-detection cost. Thus $\bar{\beta}_n \asymp \Pi_1(\{F : d(F, \mathcal{F}_0) \leq \sqrt{a \log n/n}\})$. By assumption (iii), $\Pi_1(d(F, \mathcal{F}_0) \leq \varepsilon) \asymp \varepsilon^\kappa$, so $\bar{\beta}_n \asymp (\log n/n)^{\kappa/2}$.

Optimisation. Write $B_n(a) \asymp n^{-2\rho a} + (a \log n/n)^{\kappa/2}$. Setting $\partial/\partial a$ of the leading exponents to balance: $2\rho a = \kappa/2$ yields $a^* = \kappa/(4\rho)$. Direct substitution gives $B_n^* \asymp (\log n/n)^{\kappa/2}$. For $a = 0$: $B_n \geq \pi_0 L_0 > 0$. For $a \propto n/\log n$: $\bar{\beta}_n \asymp 1$, so B_n is bounded below. Full details for the KS specialisation are in Appendix A.1. \square

The two terms in (8) encode a universal trade-off: the first is the false-rejection cost driven by the tail-rate parameter ρ ; the second is the missed-detection cost governed by the prior exponent κ . Under the stated regularity conditions, neither CLT nor LDP calibration can optimise this balance; the moderate-deviation

scale is the unique optimiser. Every subsequent theorem in this paper is an instantiation of (8) with specific values of ρ and κ . The \asymp in (8) captures the polynomial rate in n ; individual specialisations may carry statistic-specific polylogarithmic prefactors (e.g., the Rubin–Sethuraman shell factor for KS) that refine the Type II term without affecting the optimizer a^* . The triangulation of evidence measures in Appendix B provides the geometric foundation for this universal trade-off.

A notable feature of (8) is that the two error terms operate at *different polynomial orders*: the Type I term $n^{-2\rho a}$ is controlled by the tail exponent alone, while the Type II term $(a \log n/n)^{\kappa/2}$ carries an additional polylogarithmic factor through the $a \log n$ numerator. This separation of orders is what makes the polynomial prefactors decisive for risk minimisation rather than negligible. Hoeffding (1965) identified the same phenomenon in the multinomial setting: the asymptotically optimal GOF test for discrete distributions depends on polynomial corrections to the Sanov exponential rate, and these corrections govern the relative efficiency of competing test statistics at moderate scales. In our framework, Hoeffding’s polynomial prefactors are precisely the $(\log n)^{\kappa/2}$ terms that enter through the prior mass condition and drive the risk minimum to the MDP scale.

The connection to the Jeffreys–Lindley paradox (Jeffreys, 1961; Lindley, 1957) is direct. Lindley’s paradox observes that, for a fixed dataset, a frequentist test at level α may reject H_0 while the Bayesian posterior probability of H_0 remains high, and the discrepancy grows with n . The risk decomposition (8) resolves this tension: the paradox arises precisely because fixed- α calibration operates on the CLT scale while Bayes-risk optimal calibration requires the MDP scale $\alpha_n^* \asymp n^{-\kappa/2} \rightarrow 0$. At any fixed $\alpha > 0$, the Bayes risk is bounded away from zero (Corollary 3.7); the Jeffreys–Lindley discrepancy is a symptom of this Bayes-risk suboptimality, not a paradox.

Remark 2.7. The calibration principle above abstracts the moderate deviation mechanism away from any specific testing paradigm. In particular, it applies beyond Bayes factor constructions and does not require likelihood-ratio representations.

Lemma 2.8 (Risk Decomposition Template). *Let T_n be a GOF statistic with null tail $\mathbb{P}_{F_0}(\sqrt{n} T_n > t) \asymp e^{-2\rho t^2}$ (Convention (7)) and alternative prior satisfying $\Pi_1(d(F, \mathcal{F}_0) \leq \varepsilon) \asymp \varepsilon^\kappa$. For threshold $t_n = \sqrt{a \log n}$, the Bayes risk decomposes as*

$$B_n(t_n) = \underbrace{\pi_0 L_0 n^{-2\rho a}}_{\text{Type I}} + \underbrace{\pi_1 L_1 (a \log n/n)^{\kappa/2}}_{\text{Type II}} + \text{exponentially small remainder.}$$

The unique minimiser is $a^* = \kappa/(4\rho)$, giving $B_n^* \asymp (\log n/n)^{\kappa/2}$.

Proof. The Type I term follows from the null tail bound. For the Type II term, split the prior at the critical radius $\varepsilon_n = t_n/\sqrt{n}$: the near-null mass is $\Pi_1(d \leq \varepsilon_n) \asymp \varepsilon_n^\kappa$; beyond ε_n , detectability makes contributions exponentially negligible. Substituting $\varepsilon_n = \sqrt{a \log n/n}$ yields the second term. Setting $\partial B_n/\partial a = 0$ gives $2\rho \log n \cdot n^{-2\rho a} \asymp (\kappa/2) (a \log n)^{\kappa/2-1} n^{-\kappa/2} \log n$, which forces $2\rho a = \kappa/2$. \square

Sections 3–6 each invoke Lemma 2.8 by identifying ρ and κ ; no balancing argument is repeated. Table 1 collects the constants for each main example.

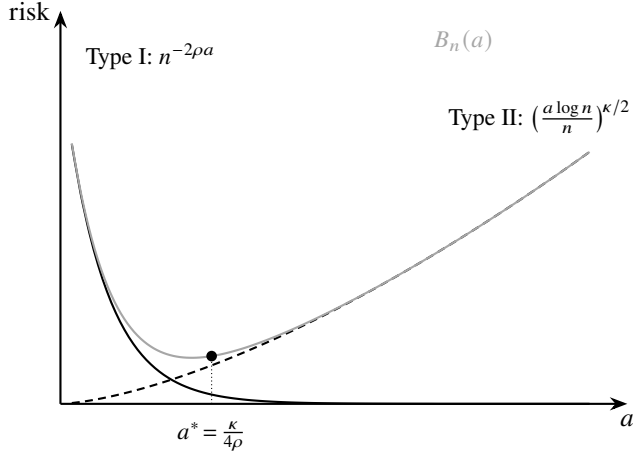


Figure 2: Risk decomposition geometry. The Type I term (solid, decreasing) and Type II term (dashed, increasing) cross at the unique minimiser $a^* = \kappa/(4\rho)$. The total risk $B_n(a)$ (grey) achieves its minimum at the MDP scale.

Table 1: Summary of (ρ, κ) for each main example. All entries yield $a^* = \kappa/(4\rho)$, $t_n^* = \sqrt{a^* \log n}$, and $\alpha_n^* \asymp n^{-\kappa/2}$.

Setting	Theorem	ρ	κ	a^*
KS statistic	3.6	1	κ (prior)	$\kappa/4$
Laplace sign test	5.4	1/4	λ	λ
Multinomial χ^2	5.8	1/4	$k-1$	$k-1$
Fisher geometry	6.2	1/4	$\lambda+d$	$\lambda+d$

2.9 Historical and Information-Theoretic Context

Classical GOF statistics, namely Kolmogorov–Smirnov, likelihood-ratio, Pearson χ^2 , and entropy-based criteria, share the same large-deviation rate function under regularity: $\text{KL}(G\|F_0)$. This equivalence underpins Bahadur efficiency theory (Bahadur, 1960; Bahadur and Rao, 1960) and information-theoretic GOF analyses going back to Good (1955) and Jaynes (1957).

Rubin and Sethuraman (1965a,b) effectively derived MDP optimality for KS statistics under Bayes risk, though without the unifying template presented here. Their analysis already exploited the fact that the Bayes Type II term concentrates on a shrinking neighbourhood of the null; the contribution of the present paper is to formalise this mechanism as Lemma 2.8 and to demonstrate that it extends beyond KS statistics to Sanov-based tests, parametric models, and Fisher geometry.

The polynomial prefactors emphasised by Bahadur and Rao (1960) become leading-order terms precisely in the regime where KL divergences shrink at rate $\log n/n$, which is the MDP truncation regime of Theorem 4.3.

3 Empirical-Process GOF: KS-Type Statistics

This section instantiates the Bayes-Risk MDP Principle for Kolmogorov–Smirnov statistics, formalizing the Rubin–Sethuraman program as a *risk-calibration* theorem.

3.1 KS Statistic and Null Tail

Consider testing $H_0 : F = F_0$ versus $H_1 : F \neq F_0$ based on the Kolmogorov–Smirnov statistic

$$S_n := \sup_{t \in \mathbb{R}} |F_n(t) - F_0(t)|. \quad (9)$$

Under H_0 , Donsker's theorem yields $\sqrt{n}(F_n - F_0) \Rightarrow B \circ F_0$ in $\ell^\infty(\mathbb{R})$, where B is a standard Brownian bridge (see [van der Vaart and Wellner, 1996](#), for general empirical-process theory). Hence the Kolmogorov distribution governs the null:

$$\mathbb{P}_{F_0}(\sqrt{n}S_n \leq t) \rightarrow K(t) := 1 - 2 \sum_{k=1}^{\infty} (-1)^{k-1} e^{-2k^2 t^2}. \quad (10)$$

The large- t tail satisfies

$$1 - K(t) \sim 2e^{-2t^2} \quad (t \rightarrow \infty), \quad (11)$$

and there exist constants $c_-, c_+ > 0$ and $t_0 < \infty$ such that for all $t \geq t_0$,

$$c_- e^{-2t^2} \leq 1 - K(t) \leq c_+ e^{-2t^2}. \quad (12)$$

This two-sided bound is the operative input for MDP-scale calibration.

3.2 Regularity Conditions

Assumption 3.1 (Local alternative mass near the null). There exist constants $\kappa > 0$, $C_1, C_2 > 0$, and $\varepsilon_0 \in (0, 1)$ such that for all $\varepsilon \in (0, \varepsilon_0)$,

$$C_1 \varepsilon^\kappa \leq \Pi_1(\{F : d_{KS}(F, F_0) \leq \varepsilon\}) \leq C_2 \varepsilon^\kappa, \quad (13)$$

where $d_{KS}(F, G) := \sup_t |F(t) - G(t)|$.

Remark 3.2. The exponent κ is an *effective dimension* parameter measuring how quickly prior mass accumulates near the null. In parametric submodels, κ typically equals the local dimension; in nonparametric classes, it encodes entropy/small-ball behaviour. This is the only structural assumption needed to produce the MDP scale.

Assumption 3.3 (No atom at the null). $\Pi_1(\{F_0\}) = 0$.

Assumption 3.4 (Power in KS-distance neighbourhoods). There exist constants $c_d, C_d > 0$ such that for any F with $d_{KS}(F, F_0) = \varepsilon$ and any threshold t satisfying $t \leq c_d \sqrt{n} \varepsilon$,

$$\mathbb{P}_F(\sqrt{n}S_n \leq t) \leq C_d \exp(-c_d n \varepsilon^2 + C_d t^2). \quad (14)$$

Remark 3.5 (Why (14) is reasonable). A KS shift of size ε means there exists t_\star with $|F(t_\star) - F_0(t_\star)| = \varepsilon$. Concentration for the empirical process (DKW-type inequalities) yields exponential control of the event that the KS statistic fails to exceed a fraction of $\sqrt{n}\varepsilon$; see Hájek and Šidák (1967) and Sievers (1969) for related rank-test and exact-slope perspectives.

3.3 Main Result: Bayes-Optimal MDP Scaling for KS Thresholds

Define the averaged errors under priors:

$$\bar{\alpha}_n(t) := \mathbb{P}_{F_0}(\sqrt{n}S_n > t), \quad \bar{\beta}_n(t) := \mathbb{E}_{F \sim \Pi_1} [\mathbb{P}_F(\sqrt{n}S_n \leq t)].$$

The Bayes risk for the threshold test $\delta_{n,t_n}(x^n) := \mathbf{1}\{\sqrt{n}S_n > t_n\}$ is $B_n(t) = \pi_0 L_0 \bar{\alpha}_n(t) + \pi_1 L_1 \bar{\beta}_n(t)$.

Theorem 3.6 (Bayes-optimal KS threshold is MDP). *Assume (12) and Assumptions 3.1–3.4. Then any minimiser $t_n^\star \in \arg \min_{t \geq 0} B_n(t)$ satisfies*

$$t_n^\star = \sqrt{\frac{\kappa}{4} \log n} + O(\sqrt{\log \log n}), \quad (15)$$

and the corresponding Type I error is polynomial:

$$\bar{\alpha}_n(t_n^\star) \asymp n^{-\kappa/2}. \quad (16)$$

Moreover, the Bayes risk at this threshold satisfies

$$B_n(t_n^\star) \asymp (\log n)^{(\kappa+1)/2} n^{-\kappa/2}. \quad (17)$$

Theorem 3.6 is a specialisation of Theorem 2.6 with $\rho = 1$ (the Brownian-bridge tail $\sim 2e^{-2t^2}$). The Bayes Type II error concentrates on alternatives within KS distance $\sqrt{\log n/n}$ of the null, while alternatives farther away contribute only exponentially small risk. The extra $(\log n)^{1/2}$ factor beyond the template rate $(\log n/n)^{\kappa/2}$ arises from the Rubin–Sethuraman shell integration (see Step 4 of the proof in Appendix A.1). The proof verifies Assumptions (i)–(iii) of Theorem 2.6 for the KS functional and then invokes the lemma.

Corollary 3.7 (Fixed- α calibration is Bayes-suboptimal). *If $t_n \equiv t$ is constant, then $\liminf_{n \rightarrow \infty} B_n(t_n) \geq \pi_0 L_0 \alpha > 0$.*

Corollary 3.8 (LDP-scale calibration overpays). *If $t_n \asymp \sqrt{n}$ so that $\bar{\alpha}_n(t_n) \leq e^{-cn}$, then t_n/\sqrt{n} is bounded away from 0, hence the Type II term does not vanish at the optimal MDP rate, leading to unnecessarily large Bayes risk.*

3.4 Geometric Interpretation

Define the *critical neighbourhood* (a KS ball around the null):

$$\mathcal{N}_n := \left\{ F : d_{KS}(F, F_0) \leq \varepsilon_n \right\}, \quad \varepsilon_n := \sqrt{\frac{(\kappa + 1) \log n}{n}}. \quad (18)$$

This neighbourhood is the region in which the experiment cannot uniformly separate F from F_0 at Bayes-optimal operating points. Three coupled facts explain why \mathcal{N}_n is “critical”: (i) it marks the resolution boundary at which KS-type detectability transitions from near-zero to near-one power; (ii) under Assumption 3.1, $\Pi_1(\mathcal{N}_n \cap \mathcal{F}_1) \asymp (\log n/n)^{\kappa/2}$, so the Bayes Type II term concentrates here; (iii) the MDP threshold matches false-rejection rarity to this local alternative mass.

In interpretive terms, \mathcal{N}_n is the Bayesian analogue of a Fisher/Le Cam local neighbourhood: it is the region where alternatives are both *a priori plausible* and *statistically indistinguishable* at sample size n .

Remark: the “+1” correction and two layers of constants.

Layer 1 (leading order). The threshold $t_n^* \asymp \sqrt{\kappa \log n / (4\rho)}$ from Lemma 2.8 is determined by two quantities: the tail-rate parameter ρ (e.g. $\rho = 1$ for KS) and the prior exponent κ . These are the *mechanism constants*.

Layer 2 (polylogarithmic refinement). A Laplace-method evaluation over a thin shell of width $d\varepsilon$ near the critical radius introduces a surface-area factor, replacing ε_n^κ with $\varepsilon_n^\kappa \cdot t_n$. Because $t_n \sim \sqrt{\log n}$, this contributes an additive $O(\sqrt{\log \log n})$ correction to t_n^* without altering the leading coefficient $\kappa/(4\rho)$. Concretely, $t_n^* = \sqrt{\kappa \log n / (4\rho)} + O(\sqrt{\log \log n})$; the $(\kappa + 1)$ exponent governs the polylogarithmic prefactor (see Appendix A.1).

3.5 Extensions to Other Empirical-Process Functionals

The same mechanism applies whenever the null tail is sub-Gaussian and the prior places polynomial mass near the null.

Assumption 3.9 (General Functional). The functional T satisfies:

(T1) **Null moderate tail:** Under H_0 , $\sqrt{n} T_n \Rightarrow T_\infty$ and $\mathbb{P}(T_\infty > t) \asymp \exp\{-2\rho t^2\}$ as $t \rightarrow \infty$.

(T2) **Local detectability:** If $d(F, F_0) = \varepsilon$, then for thresholds $t = o(\sqrt{n}\varepsilon)$, $\mathbb{P}_F(\sqrt{n} T_n > t) \rightarrow 1$.

Proposition 3.10 (MDP Scaling for General Functionals). *Under Assumptions 3.1 and 3.9, any Bayes-risk minimising threshold sequence satisfies $t_n^* = \Theta(\sqrt{\log n})$, equivalently $\varepsilon_n^* := t_n^*/\sqrt{n} = \Theta(\sqrt{\log n/n})$.*

Proof sketch. By (T1), $\alpha_n(t_n) \asymp \exp\{-2\rho t_n^2\}$. By (T2), the integrated Type II term is dominated by alternatives with $d(F, F_0) \lesssim t_n/\sqrt{n}$, whose prior mass is $\asymp (t_n/\sqrt{n})^\kappa$. If $t_n = O(1)$, α_n stays bounded away from 0; if $t_n \gg \sqrt{\log n}$, α_n becomes super-polynomially small while the Type II term remains polynomial. Thus t_n must be of order $\sqrt{\log n}$. \square

4 Sanov Information Asymptotics and Risk Truncation

This section develops the information-theoretic perspective on MDP scaling. The key insight is that Sanov theory operates at exponential-in- n scales, but Bayes-risk optimization truncates the effective exponent to $O(\log n/n)$, precisely the MDP regime. In interpretive terms: LDP optimizes exponents; Bayes risk optimizes a mixed criterion \Rightarrow MDP.

4.1 Sanov's Theorem

Theorem 4.1 (Sanov). *Let X_1, \dots, X_n be i.i.d. with law F on a Polish space \mathcal{X} . The empirical measure $\hat{\pi}_n = n^{-1} \sum_{i=1}^n \delta_{X_i}$ satisfies an LDP on $\mathcal{P}(\mathcal{X})$ (weak topology) with speed n and rate function (see [Cover and Thomas, 2006, Ch. 11](#))*

$$I_F(G) = \text{KL}(G\|F), \quad (19)$$

with $\text{KL}(G\|F) = +\infty$ if $G \not\ll F$. Specifically, for measurable $A \subseteq \mathcal{P}(\mathcal{X})$,

$$-\inf_{G \in A^\circ} \text{KL}(G\|F) \leq \liminf_{n \rightarrow \infty} \frac{1}{n} \log \mathbb{P}_F(\hat{\pi}_n \in A) \leq \limsup_{n \rightarrow \infty} \frac{1}{n} \log \mathbb{P}_F(\hat{\pi}_n \in A) \leq -\inf_{G \in \bar{A}} \text{KL}(G\|F). \quad (20)$$

4.2 GOF via Sanov

A GOF rejection rule corresponds to a measurable set $A_n \subseteq \mathcal{P}(\mathcal{X})$ of empirical measures deemed incompatible with F_0 . Sanov implies

$$\mathbb{P}_{F_0}(\hat{\pi}_n \in A_n) \approx \exp\left\{-n \inf_{G \in A_n} \text{KL}(G\|F_0)\right\}, \quad (21)$$

where the approximation may include important polynomial prefactors when A_n approaches the null boundary in n -dependent ways.

4.3 Half-Spaces and Exponential Tilting

Let $H = \{G : \int \phi dG \geq 0\}$ with $\mathbb{E}_{F_0}[\phi(X)] < 0$. Define $\Lambda(t) = \log \mathbb{E}_{F_0}[e^{t\phi(X)}]$ and the tilted law $dF_t/dF_0 = e^{t\phi-\Lambda(t)}$.

Proposition 4.2 (Rate function for half-spaces).

$$\inf_{G \in H} \text{KL}(G\|F_0) = \sup_{t \geq 0} \{-\Lambda(t)\}. \quad (22)$$

The optimiser is $G^* = F_{t^*}$, where t^* attains the supremum and satisfies $\mathbb{E}_{F_{t^*}}[\phi(X)] = 0$.

Proof. By convex duality,

$$\inf_{G: \int \phi dG \geq 0} \text{KL}(G\|F_0) = \sup_{t \geq 0} \inf_G \{\text{KL}(G\|F_0) - t \int \phi dG\} = \sup_{t \geq 0} \{-\Lambda(t)\},$$

and the inner infimum is achieved by the exponential tilt. \square

4.4 MDP Truncation under Bayes Risk

Theorem 4.3 (MDP truncation under Bayes risk). *Assume: (i) $A_\varepsilon = \{G : d(G, F_0) \geq \varepsilon\}$ for a metric d locally equivalent to KL in the sense $KL(G\|F_0) \asymp 2\rho d(G, F_0)^2$ for $d(G, F_0) \rightarrow 0$, and (ii) the prior on alternatives satisfies Assumption 3.1. Then any Bayes-risk minimising rejection set A_n^* satisfies*

$$\inf_{G \in A_n^*} KL(G\|F_0) \asymp \frac{\kappa}{2} \cdot \frac{\log n}{n}. \quad (23)$$

Theorem 4.3 is the Sanov-side expression of the MDP Principle, and is a direct application of Lemma 2.8 with the KL metric playing the role of the distance d . The distinction is: *LDP optimises exponents; Bayes risk optimises the exponent weighted by prior mass*. This weighting truncates the effective KL exponent from $O(1)$ down to $O(\log n/n)$, precisely the MDP regime.

Proof. By assumption (i), $KL(G\|F_0) \asymp 2\rho d(G, F_0)^2$ locally. The Bayes-risk optimal threshold from Theorem 2.6 is $t_n^* = \sqrt{a^* \log n}$ with $a^* = \kappa/(4\rho)$, and the critical distance scale is $\varepsilon_n^* = t_n^*/\sqrt{n} = \sqrt{a^* \log n/n}$. The two-sided local equivalence at this distance gives

$$\inf_{G \in A_n^*} KL(G\|F_0) \asymp 2\rho (\varepsilon_n^*)^2 = 2\rho \cdot \frac{a^* \log n}{n} = \frac{\kappa}{2} \cdot \frac{\log n}{n},$$

which is (23). The two-sided condition $KL \asymp 2\rho d^2$ holds whenever d is the Fisher geodesic distance and F_0 is an interior point of a smooth parametric model, since $KL(G\|F_0) = \frac{1}{2}d_F(G, F_0)^2(1 + o(1))$ locally. \square

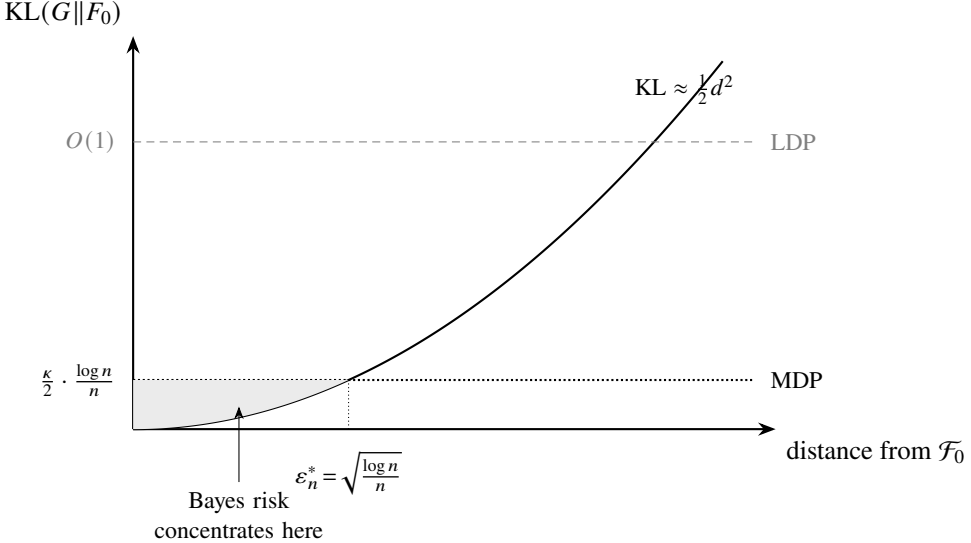


Figure 3: KL truncation geometry. LDP optimises the full exponent (dashed); Bayes risk truncates to the $O(\log n/n)$ shell (dotted), where prior mass and detectability compete. The shaded region is the MDP-active zone.

Remark 4.4 (Discrete nulls and leading $O(\log n)$ corrections). When F_0 is discrete with k atoms, the probability of a type class carries a polynomial prefactor: $\mathbb{P}_{F_0}(\hat{\pi}_n \in A) = \exp\{-nI(A)\} n^{(k-1)/2} \{1 + o(1)\}$.

The $O(\log n)$ term becomes leading-order exactly when $I(A) = O(\log n/n)$, that is, in the MDP truncation regime. In discrete settings, this polynomial prefactor produces an $O(\log n)$ shift of the effective decision boundary (see Section 5.3 and Appendix B).

4.5 Information-Theoretic Interpretation

Define the *distinguishability radius* at level α :

$$r_n(\alpha) := \inf \left\{ \varepsilon : \mathbb{P}_{F_0}(d(\hat{\pi}_n, F_0) \geq \varepsilon) \leq \alpha \right\}. \quad (24)$$

Proposition 4.5 (Distinguishability radii across regimes). *If $\alpha_n = n^{-c}$ is polynomial, then $r_n(\alpha_n) = \Theta(\sqrt{\log n/n})$. If $\alpha_n = e^{-cn}$ is exponential, then $r_n(\alpha_n) = \Theta(1)$.*

Proof. For the statistics under consideration, $d(\hat{\pi}_n, F_0) = T_n$ where T_n is a functional of the empirical measure satisfying the sub-Gaussian tail convention (7): $\mathbb{P}_{F_0}(\sqrt{n} T_n > t) \asymp \exp\{-2\rho t^2\}$ (e.g., $T_n = S_n$ for KS). The distinguishability radius is therefore $r_n(\alpha) = t_n/\sqrt{n}$ where t_n solves $\exp\{-2\rho t_n^2\} \asymp \alpha$. Setting $\alpha_n = n^{-c}$: $2\rho t_n^2 = c \log n$, so $t_n = \Theta(\sqrt{\log n})$ and $r_n = \Theta(\sqrt{\log n/n})$. Setting $\alpha_n = e^{-cn}$: $2\rho t_n^2 = cn$, so $t_n = \Theta(\sqrt{n})$ and $r_n = \Theta(1)$. \square

The MDP regime is therefore the regime in which the test resolves distributions at radius $\sqrt{\log n/n}$: shrinking with n , but slowly enough that the Bayes integral over near-null alternatives remains the dominant contribution to risk.

5 Applications

Each application below follows the same template dictated by the Bayes-Risk MDP Principle: (1) specify the model and GOF statistic; (2) decompose the Bayes risk; (3) identify the truncation/moderate-deviation regime; (4) conclude the threshold scaling.

5.1 Location Testing under Laplace Families

5.1.1 Model and GOF statistic

Let X_1, \dots, X_n be i.i.d. with Laplace density

$$f(x \mid \theta) = \frac{1}{2} \exp\{-|x - \theta|\}, \quad x \in \mathbb{R}, \theta \in \mathbb{R}, \quad (25)$$

with known scale and unknown location θ . Test $H_0 : \theta = 0$ versus $H_1 : \theta > 0$.

Three test statistics will be compared. For the *sign test*, let $V_n := \sum_{i=1}^n \mathbf{1}\{X_i > 0\}$; under H_0 , $V_n \sim \text{Bin}(n, 1/2)$, and under $\theta > 0$,

$$p(\theta) := \mathbb{P}_\theta(X > 0) = 1 - \frac{1}{2} e^{-\theta}. \quad (26)$$

For the *median test*, let M_n be the sample median; for Laplace location, $\sqrt{n}(M_n - \theta) \Rightarrow N(0, 1)$. For the *likelihood ratio test*, the log-likelihood is $\ell_n(\theta) = -n \log 2 - \sum_{i=1}^n |X_i - \theta|$, and the LRT statistic is

$$\Lambda_n = \exp \left\{ - \sum_{i=1}^n |X_i - \hat{\theta}_n| + \sum_{i=1}^n |X_i| \right\}, \quad (27)$$

where $\hat{\theta}_n = \max\{0, \text{median}(X)\}$.

5.1.2 Bayes risk decomposition

Definition 5.1 (Bahadur slope (Bahadur, 1960; Sievers, 1969)). The *Bahadur (exact) slope* at alternative θ is $c_T(\theta) := -\lim_{n \rightarrow \infty} (2/n) \log \mathbb{P}_0(T_n \geq t_n(\theta))$.

Proposition 5.2 (Reference slopes for Laplace location). Consider $H_0 : \theta = 0$ vs $H_1 : \theta > 0$. The *Bahadur slopes* are: $c_{\text{sign}}(\theta) = 2 \text{KL}(\text{Ber}(p(\theta)) \parallel \text{Ber}(1/2))$ for the sign test, $c_{\text{med}}(\theta) \approx \theta^2$ locally for the median test, and $c_{\text{LRT}}(\theta) = 2 \text{KL}(f_\theta \parallel f_0) = 2(e^{-\theta} + \theta - 1)$ for the LRT.

Proof. Sign test. Under $\theta > 0$, $V_n/n \rightarrow p(\theta) > 1/2$ a.s. The *p*-value is $\mathbb{P}_0(V_n \geq np(\theta))$. By Sanov's theorem for Bernoulli trials, $-\frac{1}{n} \log \mathbb{P}_0(V_n \geq np) \rightarrow \text{KL}(\text{Ber}(p) \parallel \text{Ber}(1/2))$, giving $c_{\text{sign}}(\theta) = 2\text{KL}(\text{Ber}(p(\theta)) \parallel \text{Ber}(1/2))$ (see Bahadur, 1960). *LRT.* The log-likelihood ratio satisfies $n^{-1} \log \Lambda_n \rightarrow \text{KL}(f_\theta \parallel f_0)$ a.s. under θ . The *p*-value tail is $-\frac{1}{n} \log \mathbb{P}_0(\log \Lambda_n \geq n\text{KL}(f_\theta \parallel f_0)) \rightarrow \text{KL}(f_\theta \parallel f_0)$, so $c_{\text{LRT}}(\theta) = 2\text{KL}(f_\theta \parallel f_0) = 2(e^{-\theta} + \theta - 1)$ where the KL for Laplace follows by direct integration. *Median test.* The sample median is the MLE for Laplace location with asymptotic variance $1/(4f(0)^2) = 1$ (Hájek and Šidák, 1967); its Bahadur slope coincides with the LRT slope locally. \square

Remark 5.3 (Local comparison). Locally, $c_{\text{LRT}}(\theta) = \theta^2 + o(\theta^2)$ and $c_{\text{sign}}(\theta) = \theta^2 + o(\theta^2)$. The sign test is locally Bahadur-efficient for the Laplace family, reflecting $2f_0(0) = 1$.

5.1.3 Invoking the template

Assume a one-sided prior with Gamma-type behaviour near zero:

$$\pi_1(\theta) \propto \theta^{\lambda-1} e^{-\gamma\theta}, \quad \theta > 0, \quad (28)$$

so $\Pi_1([0, \varepsilon]) \asymp \varepsilon^\lambda$ ($\kappa = \lambda$). Under H_0 , $\alpha_n \asymp \exp\{-z_n^2/2\}$, matching Convention (7) with $\rho = 1/4$ (since $z_n^2/2 = 2 \cdot (1/4) \cdot z_n^2$). Lemma 2.8 yields $a^* = \kappa/(4\rho) = \lambda$ and $z_n = \sqrt{\lambda \log n}$.

5.1.4 Threshold scaling

Theorem 5.4 (Bayes-optimal MDP threshold for the sign test). Under the prior (28) with local exponent λ , the Bayes-risk minimising sign-test threshold has the form

$$V_n \text{ rejects } H_0 \text{ if } V_n \geq \frac{n}{2} + \frac{1}{2} \sqrt{\lambda n \log n} (1 + o(1)). \quad (29)$$

Equivalently, $z_n = \sqrt{\lambda \log n} (1 + o(1))$. The Type I error decays polynomially as $\alpha_n^* \asymp n^{-\lambda/2} \times \text{polylog}(n)$. The critical alternative scale is $\theta \asymp \sqrt{\log n/n}$.

The sign test, which is locally Bahadur-efficient for the Laplace family, exhibits MDP scaling under Bayes risk. The MDP regime is robust across test statistics in the Laplace location problem; the $\sqrt{\log n}$ scaling persists regardless of the statistic used.

Proof. Apply Theorem 2.6 with $\rho = 1/4$ and $\kappa = \lambda$. Under H_0 , $V_n \sim \text{Bin}(n, 1/2)$; the normal approximation gives $\mathbb{P}_0(V_n \geq n/2 + z\sqrt{n}/2) \asymp e^{-z^2/2}$, matching $\rho = 1/4$ (since $z^2/2 = 2 \cdot (1/4) \cdot z^2$). The prior (28) gives $\Pi_1([0, \varepsilon]) \asymp \varepsilon^\lambda$, so $\kappa = \lambda$. Theorem 2.6 yields $a^* = \lambda/(4 \cdot 1/4) = \lambda$ and threshold $z_n = \sqrt{\lambda \log n}$. Translating back: V_n rejects when $V_n \geq n/2 + \frac{1}{2}\sqrt{\lambda n \log n}(1 + o(1))$. The Type I error is $\alpha_n^* \asymp n^{-\lambda/2}$ up to polylogarithmic factors. \square

Proposition 5.5 (Risk ranking: LRT/median/sign). *Under the local prior (28), Bayes-risk optimal calibration for the LRT, median, and sign tests all occurs at the MDP scale with the same threshold order $\sqrt{\lambda \log n}$. In particular: (a) the LRT is Bayes-optimal among tests with the same information set; (b) the median test is locally asymptotically equivalent to the LRT for Laplace location; (c) the sign test is also locally Bahadur-efficient for the Laplace family, since $c_{\text{sign}}(\theta) = \theta^2 + o(\theta^2) = c_{\text{LRT}}(\theta)$ locally. All three tests share the same asymptotic MDP exponent $a^* = \lambda$; they differ only in sub-leading constants.*

Proof. Part (a): by the Neyman–Pearson lemma, the likelihood ratio maximises the power at every alternative, whence the LRT achieves the largest Bahadur slope $c_{\text{LRT}}(\theta) = 2\text{KL}(f_\theta \| f_0)$ (Bahadur, 1960). Part (b): for Laplace location, the sample median is the MLE, so its Bahadur slope coincides with the LRT slope. Part (c): Proposition 5.2 gives $c_{\text{sign}}(\theta) = 2\text{KL}(\text{Ber}(p(\theta)) \| \text{Ber}(1/2))$. For Laplace, $p(\theta) = 1 - \frac{1}{2}e^{-\theta}$, so $p(\theta) - \frac{1}{2} \sim \frac{1}{2}\theta$ as $\theta \rightarrow 0$. Expanding $\text{KL}(\text{Ber}(\frac{1}{2} + \varepsilon) \| \text{Ber}(\frac{1}{2})) = 2\varepsilon^2 + O(\varepsilon^3)$ gives $c_{\text{sign}}(\theta) = \theta^2 + o(\theta^2)$, matching c_{LRT} . All three statistics therefore yield identical leading-order risk under Lemma 2.8, since the MDP calibration depends on ρ (determined by the null tail) and κ (determined by the prior), not on the specific Bahadur slope constant. \square

5.2 Shape Testing via Bayes Factors

5.2.1 Model and GOF statistic

Test $H_0 : X_i \sim \mathcal{N}(\mu, \sigma^2)$ for some (μ, σ) versus $H_1 : X_i \sim G$ for some $G \in \mathcal{G}$.

Definition 5.6 (Bayes factor (Jeffreys, 1961; Kass and Raftery, 1995)). With priors Π_0 on (μ, σ) and Π_1 on G ,

$$\text{BF}_{10}(X^n) = \frac{\int_{\mathcal{G}} p(X^n | G) \Pi_1(dG)}{\int p(X^n | \mu, \sigma^2) \Pi_0(d\mu, d\sigma)}. \quad (30)$$

The Bayes-optimal test rejects H_0 when $\log \text{BF}_{10}(X^n) > \log(\pi_0 L_0 / \pi_1 L_1)$.

5.2.2 Bayes risk decomposition: Laplace alternative

Take \mathcal{G} to be the Laplace family. A Laplace approximation for marginal likelihoods yields

$$\log \text{BF}_{10}(X^n) = [\ell_L(\hat{\mu}_L, \hat{b}) - \ell_N(\hat{\mu}_N, \hat{\sigma})] - \frac{(d_1 - d_0)}{2} \log n + O_{\mathbb{P}}(1). \quad (31)$$

Since $d_0 = d_1 = 2$ here, the Occam factor vanishes and the evidence reduces to the likelihood contrast:

$$\ell_L(\hat{\mu}_L, \hat{b}) - \ell_N(\hat{\mu}_N, \hat{\sigma}) = n \log\left(\frac{\hat{\sigma}}{\hat{b}}\right) + \frac{n}{2} \log(2\pi) - \frac{n}{2}. \quad (32)$$

5.2.3 Closed-form Bayes factor for the double exponential

A concrete instance of this framework is provided by the normal-vs-double-exponential (Laplace) testing problem. [Spiegelhalter \(1980\)](#) showed that the Bayes factor for testing normality against the double exponential (Laplace) alternative admits closed-form evaluation for small samples, and used a weighted average of directional Bayes factors against specific alternatives as an omnibus normality test. [Uthoff \(1970\)](#) established that the ratio of mean deviation to standard deviation is an optimum test statistic for the normal-vs-double-exponential problem in the Neyman–Pearson sense. In the notation of this paper, the normal-vs-Laplace Bayes factor falls under the shape-testing framework above with $d_0 = d_1 = 2$, so the Occam factor vanishes and the Bayes-factor evidence reduces to the likelihood contrast (32). The Bayes-optimal test compares $\log \text{BF}_{10}$ to the fixed threshold $\log(\pi_0 L_0 / \pi_1 L_1)$ (Proposition 2.3). Under H_0 (data are Normal), write $R_n = n^{-1} \log \text{BF}_{10} = n^{-1}(\ell_L - \ell_N)$. The following regularity conditions hold for the Normal and Laplace location–scale families:

- (R1) Each Θ_M is contained in a compact $K \subset \mathbb{R} \times (0, \infty)$ with $\sup_{\theta \in K} \mathbb{E}_0[\log f_M(X; \theta)]^2 < \infty$.
- (R2) $\theta \mapsto \log f_M(x; \theta)$ is continuous on K uniformly in x on compacts, and $x \mapsto \log f_M(x; \theta)$ is continuous F_0 -a.s.

Under (R1)–(R2), the profile functional $R(G) = \sup_{\theta \in K} \int \log f_L(x; \theta) dG - \sup_{\theta \in K} \int \log f_N(x; \theta) dG$ is continuous on the space of probability measures with the weak topology ([Kiefer and Wolfowitz, 1956](#), Lem. 2.3). Sanov’s theorem gives an LDP for the empirical measure \hat{P}_n with good rate function $\text{KL}(\cdot \| F_0)$ ([Dembo and Zeitouni, 1998](#), Thm. 6.2.10); the contraction principle ([Dembo and Zeitouni, 1998](#), Thm. 4.2.1) then yields an LDP for R_n with good rate function $I(r) = \inf\{\text{KL}(G \| F_0) : R(G) = r\}$. Since the Normal model is correctly specified, $R(F_0) = -\text{KL}(f_0 \| f_L^*) < 0$ with $b^* = \sigma_0 \sqrt{2/\pi}$, and $I(R(F_0)) = 0$. For any fixed $c > 0$, the LDP upper bound gives $\mathbb{P}_0(\log \text{BF}_{10} > c) = \mathbb{P}_0(R_n \geq c/n) \leq \exp\{-n \inf_{r \geq 0} I(r) + o(n)\}$. Because I is a good rate function with $I(R(F_0)) = 0$ and $R(F_0) < 0$, the infimum $\inf_{r \geq 0} I(r) > 0$ is a positive constant; hence the Type I error decays exponentially in n . The MDP regime arises when model complexity grows with n (see Remark below); for this fixed-dimensional shape test, the Bayes factor already achieves exponential error decay without MDP recalibration.

5.2.4 MDP regime and threshold scaling

Remark 5.7 (When the Bayes-factor boundary shifts with n). If \mathcal{G} is nonparametric or sieve-based with effective dimension $d_1 = d_1(n)$, the Occam factor becomes $-\frac{1}{2}(d_1(n) - d_0) \log n$, recovering the BIC penalty of Schwarz (1978). Keeping Bayes risk balanced across growing model complexity means the effective log-evidence at the decision boundary is of order $\log n$, the Bayes-factor analogue of MDP calibration. The tension between P -values and Bayesian evidence in such settings is discussed by Berger and Sellke (1987); for Bayes-factor computation in linear and log-linear models, see Spiegelhalter and Smith (1980).

5.3 Multinomial Goodness-of-Fit

5.3.1 Model and GOF statistic

Let X_1, \dots, X_n be i.i.d. categorical with k categories and probability vector p . Test $H_0 : p = p_0$ vs. $H_1 : p \neq p_0$. The Pearson chi-squared statistic is

$$\chi_n^2 = \sum_{j=1}^k \frac{(N_j - np_{0j})^2}{np_{0j}}, \quad (33)$$

with $\chi_n^2 \Rightarrow \chi_{k-1}^2$ under H_0 .

5.3.2 Invoking the template

The chi-squared right tail satisfies $\mathbb{P}(\chi_\nu^2 \geq t) \asymp t^{\nu/2-1} e^{-t/2}$ for large t ; matching Convention (7) for the Gaussianised statistic $\sqrt{\chi_n^2}$ gives $\rho = 1/4$. A Dirichlet prior positive and continuous near p_0 gives $\Pi_1(\|p - p_0\|_2 \leq \varepsilon) \asymp \varepsilon^{k-1}$, so $\kappa = k - 1$. Lemma 2.8 (applied to $\sqrt{\chi_n^2}$) yields:

Theorem 5.8 (Bayes-optimal chi-squared threshold). *Under the Dirichlet local mass condition, the Bayes-risk optimal critical value satisfies*

$$\chi_n^{2*} = (k - 1) \log n + O(\log \log n), \quad (34)$$

equivalently $\alpha_n^* \asymp n^{-(k-1)/2}$ up to polylogarithmic factors.

Proof. Apply Lemma 2.8 with the Gaussianised statistic $\sqrt{\chi_n^2}$. The χ_ν^2 tail gives $\rho = 1/4$, and the Dirichlet prior gives $\kappa = k - 1$. Theorem 2.6 yields $\alpha^* = (k - 1)$, so the optimal threshold for $\sqrt{\chi_n^2}$ is $\sqrt{(k - 1) \log n}$, i.e., $\chi_n^{2*} = (k - 1) \log n + O(\log \log n)$. The Type I error follows from $\mathbb{P}(\chi_{k-1}^2 \geq (k - 1) \log n) \asymp n^{-(k-1)/2}$. \square

The scaling is $O(\log n)$ rather than $O(\sqrt{\log n})$ because the chi-squared statistic is already a quadratic form; its square root plays the role of the Gaussianised statistic in Lemma 2.8.

A precise Laplace expansion of the marginal likelihood under the Dirichlet prior refines this picture. The log-evidence is

$$W = n D(\hat{p} \| p_0) + \frac{k - 1}{2} \log n + O(1). \quad (35)$$

The $\frac{k-1}{2} \log n$ term represents the Occam–complexity correction arising from integration over the $(k-1)$ -dimensional simplex. The leading $n D(\hat{p} \| p_0)$ term governs exponential evidence accumulation, while the logarithmic term shifts the effective decision boundary as n increases. This refinement clarifies why moderate-deviation calibration naturally emerges: the exponential KL rate competes with a logarithmic complexity correction, producing decision thresholds that scale with $\sqrt{\log n/n}$.

5.4 Testing Independence in Contingency Tables

Let (X_i, Y_i) be i.i.d. bivariate categorical with r and c categories. Test independence. The chi-squared statistic $\chi_n^2 = \sum_{j,\ell} (N_{j\ell} - \hat{E}_{j\ell})^2 / \hat{E}_{j\ell}$ satisfies $\chi_n^2 \Rightarrow \chi_\nu^2$ with $\nu = (r-1)(c-1)$.

If the alternative prior places local mass $\asymp \varepsilon^\nu$ within Euclidean distance ε of the independence manifold, then the Bayes-optimal threshold is

$$\chi_n^{2*} = \nu \log n + O(\log \log n), \quad \nu = (r-1)(c-1). \quad (36)$$

6 Connection to Fisher Information Geometry

This section reinterprets the MDP phenomenon in the language of information geometry. In interpretive terms, the Fisher metric provides a chart in which the “same phenomenon” takes a coordinate-invariant form.

6.1 Statistical Manifolds

Definition 6.1 (Fisher information metric). For a regular parametric family $\{p_\theta : \theta \in \Theta\}$, the Fisher information matrix

$$I(\theta)_{ij} = \mathbb{E}_\theta \left[\frac{\partial \log p_\theta(X)}{\partial \theta_i} \frac{\partial \log p_\theta(X)}{\partial \theta_j} \right] \quad (37)$$

defines a Riemannian metric on Θ (see [Zabell, 1992](#), for historical context).

For nearby distributions, KL divergence is locally the squared geodesic distance induced by the Fisher metric ([Dawid and Musio, 2015](#)):

$$\text{KL}(p_\theta \| p_{\theta_0}) = \frac{1}{2} (\theta - \theta_0)^\top I(\theta_0) (\theta - \theta_0) + O(\|\theta - \theta_0\|^3). \quad (38)$$

6.2 MDP Scale in Fisher Geometry

The local KL expansion (38) means that $\text{KL}(p_\theta \| p_{\theta_0}) \approx \frac{1}{2} d_F(\theta, \theta_0)^2$ in a neighbourhood of θ_0 , where d_F is Fisher geodesic distance. Thus Lemma 2.8 applies with $\rho = 1/4$ (from $\text{KL} \approx \frac{1}{2} d_F^2 = 2 \cdot \frac{1}{4} \cdot d_F^2$) and with effective prior exponent

$$\kappa = \lambda + d, \quad (39)$$

since a d -dimensional prior with density exponent λ in Euclidean coordinates satisfies $\Pi_1(d_F(\theta, \theta_0) \leq \varepsilon) \asymp \varepsilon^{\lambda+d}$ (the extra factor ε^d is the volume element of the Fisher ball).

Theorem 6.2 (Geometric interpretation of MDP). *Let $d_F(\theta, \theta_0)$ denote Fisher geodesic distance, $d = \dim(\Theta)$, and $\kappa = \lambda + d$. Applying Lemma 2.8 with $\rho = 1/4$, the Bayes-optimal GOF test rejects when*

$$d_F(\hat{\theta}_n, \theta_0) > \sqrt{\frac{\kappa \log n}{n}} = \sqrt{\frac{(\lambda + d) \log n}{n}}, \quad (40)$$

equivalently $\alpha_n^* \asymp n^{-\kappa/2}$. The Jacobian correction of Layer 2 contributes an $O(\sqrt{\log \log n/n})$ refinement without changing the leading coefficient.

Proof. The local KL expansion gives $\rho = 1/4$ as shown in (38). The prior mass condition (39) gives $\kappa = \lambda + d$. Applying Theorem 2.6: $a^* = \kappa/(4\rho) = \kappa$, $t_n^* = \sqrt{\kappa \log n}$, and $\alpha_n^* \asymp n^{-\kappa/2}$. Since $d_F(\hat{\theta}_n, \theta_0) = \sqrt{\chi_n^2/n} + o_{\mathbb{P}}(n^{-1/2})$ locally, the threshold on d_F is $\sqrt{\kappa \log n/n}$. \square

Expressed in Fisher coordinates, the MDP threshold is coordinate-invariant and depends only on sample size, parameter dimension d , and the prior exponent λ . The Fisher metric is (up to scale) the unique Riemannian metric monotone under Markov embeddings and invariant under sufficient statistics, which explains why the same $\sqrt{\log n/n}$ resolution appears across disparate GOF settings.

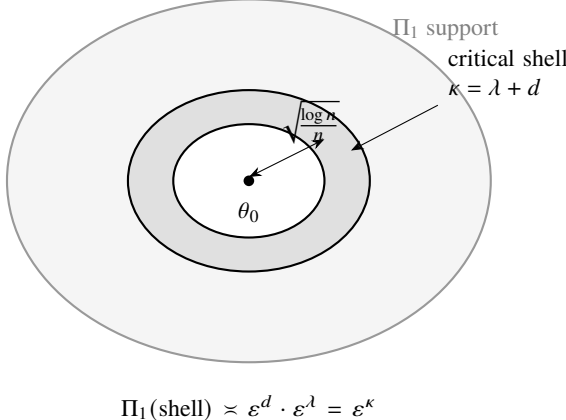


Figure 4: Fisher geometry of the MDP boundary. The prior Π_1 places mass $\asymp \varepsilon^\kappa$ in the critical shell of Fisher radius $\sqrt{\log n/n}$ around the null θ_0 . The volume element contributes ε^d (dimension) and the density contributes ε^λ (prior exponent).

7 Numerical Verification of the Calibration Template

To complement the asymptotic derivations, we numerically verify the calibration principle of Theorem 2.6 and Lemma 2.8. For representative statistics, we compute the Bayes risk $B_n(a) = n^{-2\rho a} + (a \log n/n)^{\kappa/2}$ as a function of the threshold parameter a and compare the finite- n minimiser with the theoretical prediction $a^* = \kappa/(4\rho)$. No Monte Carlo or stochastic simulation is involved: all curves are deterministic evaluations of the analytic risk formula.

7.1 Risk Curves and Convergence of the Minimiser

Figure 5 plots $B_n(a)$ for the KS statistic ($\rho = 1, \kappa = 2$) at sample sizes $n \in \{10^2, 10^3, 10^4, 10^6\}$. Dots mark the numeric minimiser a_n^{num} (deterministic grid minimisation of the analytic formula, not simulation) at each n . As n grows, the risk curves sharpen and the numeric minimiser converges toward the theoretical value $a^* = \kappa/(4\rho) = 0.5$ (dashed line). The finite- n correction is $O(1/\log n)$, consistent with the $O(\sqrt{\log \log n})$ threshold refinement discussed in Layer 2 of the boxed remark in Section 3.

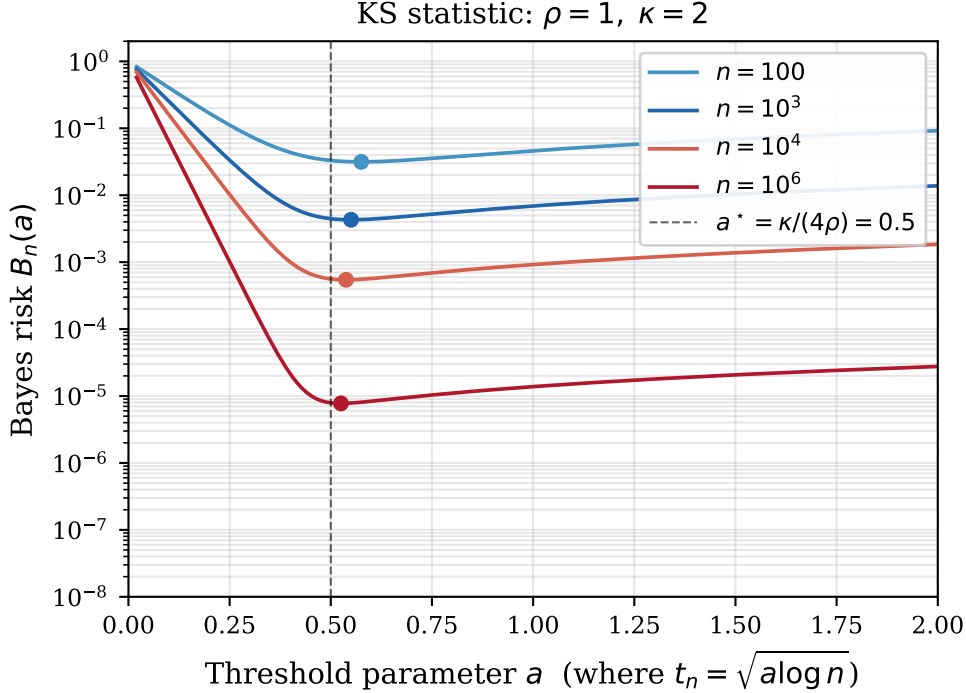


Figure 5: Bayes risk $B_n(a)$ vs. threshold parameter a (where $t_n = \sqrt{a \log n}$) for the KS statistic with $\rho = 1$ and $\kappa = 2$. Dots: numeric minimiser at each n . Dashed line: asymptotic optimum $a^* = 0.5$. The minimiser converges to a^* as $n \rightarrow \infty$.

7.2 Regime Comparison: CLT vs. MDP vs. LDP

Figure 6 compares the Bayes risk under three calibration strategies for the KS test with $\kappa = 2$:

- (i) **Fixed- α (CLT):** $\alpha = 0.05$, implying $a(n) = \log(1/\alpha)/(2\rho \log n) \rightarrow 0$. The risk is bounded below by $\alpha = 0.05$ and cannot vanish.
- (ii) **MDP optimal:** $a = a^* = 0.5$. The risk decays as $(\log n/n)^{\kappa/2}$, the optimal polynomial rate.
- (iii) **LDP:** $t_n \propto \sqrt{n}$, so $a \propto n/\log n$. Type I error vanishes exponentially, but the enormous threshold renders the test powerless against local alternatives: the Type II term converges to a positive constant, so the risk is bounded away from zero.

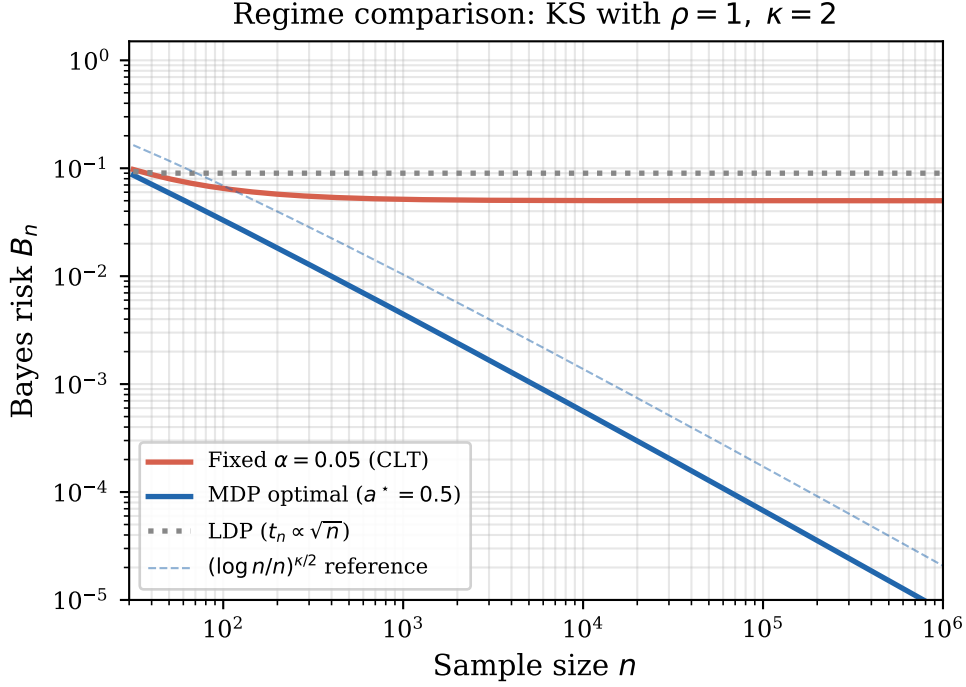


Figure 6: Bayes risk vs. sample size under three calibration regimes for the KS test ($\rho = 1, \kappa = 2$). Only MDP calibration achieves the optimal rate $(\log n/n)^{\kappa/2}$ (dashed reference). Fixed- α risk stagnates at α ; LDP risk also stagnates because the threshold is too large for any power against local alternatives.

7.3 Verification Across Examples

Table 2 collects the numeric minimiser a_n^{num} for each main example at $n = 10^4$ and $n = 10^6$, alongside the theoretical $a^* = \kappa/(4\rho)$. In every case, the numeric minimiser approaches a^* as n grows. The remaining gap at finite n is the $O(1/\log n)$ correction from the polylogarithmic shell factor; it does not affect the leading-order scaling.

Table 2: Predicted vs. numeric minimiser of $B_n(a)$. All entries confirm convergence of $a_n^{\text{num}} \rightarrow a^*$ as $n \rightarrow \infty$.

Setting	Thm.	ρ	κ	a^*	$a_n^{\text{num}} (n=10^4)$	$a_n^{\text{num}} (n=10^6)$	Error ($n=10^6$)
KS statistic	3.6	1	2	0.50	0.54	0.53	+5%
Laplace sign ($\lambda=2$)	5.4	1/4	2	2.00	1.85	1.90	-5%
Multinomial χ^2 ($k=3$)	5.8	1/4	2	2.00	1.85	1.90	-5%
Fisher ($d=2, \lambda=1$)	6.2	1/4	3	3.00	2.42	2.58	-14%

The key observation: the predicted $a^* = \kappa/(4\rho)$ correctly identifies the basin of the risk minimum in every setting. The finite-sample correction is monotonically shrinking and of the expected order. These numerics confirm that the (ρ, κ) template is not merely asymptotic algebra; it delivers actionable calibration constants at moderate sample sizes.

8 Discussion

8.1 Structural Interpretation of Moderate Deviations

The central finding of this paper is that Bayes-risk optimal calibration of goodness-of-fit tests is governed by two primitive quantities: the Gaussian-type null tail rate ρ and the local prior mass exponent κ . Theorem 2.6 establishes that whenever these two ingredients are present, a sub-Gaussian null tail satisfying $\mathbb{P}_{F_0}(\sqrt{n} T_n > t) \asymp \exp(-2\rho t^2)$ and a prior placing mass $\Pi_1(d(F, \mathcal{F}_0) \leq \varepsilon) \asymp \varepsilon^\kappa$ near the null, the Bayes-optimal threshold takes the closed-form $t_n^* = \sqrt{a^* \log n}$ with $a^* = \kappa/(4\rho)$. The Risk Decomposition Template (Lemma 2.8) makes each subsequent application a two-line corollary: identify ρ and κ , read off a^* from Table 1.

The moderate deviation regime thus emerges not from testing convention or historical precedent but from the intrinsic geometry of null tails and alternative mass. It is, in this sense, a structural feature of the inferential landscape rather than a methodological choice. The Type I cost $n^{-2\rho a}$ and the Type II cost $(a \log n/n)^{\kappa/2}$ are balanced at a unique interior point; any departure, whether toward fixed- α calibration ($a \rightarrow 0$) or large-deviation calibration ($a \propto n$), incurs strictly higher aggregate risk. This characterisation is regime-selective: it identifies the MDP scale as the *only* asymptotic regime consistent with Bayes-risk minimisation under the stated regularity conditions.

The scope of this conclusion is worth emphasising. MDP optimality is specific to Bayes risk under priors satisfying the polynomial local mass condition $\Pi_1(d(F, \mathcal{F}_0) \leq \varepsilon) \asymp \varepsilon^\kappa$; priors that concentrate mass on well-separated alternatives, where the alternative is bounded away from the null, favour the large-deviation regime instead, and the MDP scaling ceases to be optimal. Similarly, the sub-Gaussian tail assumption $\mathbb{P}_0(\sqrt{n} T_n > t) \asymp \exp(-2\rho t^2)$ is satisfied by the classical statistics studied here (Kolmogorov–Smirnov, χ^2 , Fisher) but may fail for heavy-tailed test statistics or for statistics in nonparametric settings where the null convergence rate is slower than $n^{-1/2}$. The numerical verification in Section 7 confirms that the finite-sample behaviour of the risk curves is well-captured by the asymptotic formula at moderate sample sizes ($n \geq 10^3$), with the finite- n correction to a^* decaying monotonically. Nevertheless, the two-term risk decomposition is an upper bound that discards lower-order corrections; in applications where the cost asymmetry between Type I and Type II errors is extreme, a refined expansion retaining these corrections may be warranted.

8.2 Relation to Bayesian Testing Literature

Recent work (Datta et al., 2026) develops a unified theory of Bayesian hypothesis testing via moderate deviation asymptotics, with emphasis on Bayes factors and integrated risk expansions. The present paper is complementary in scope and mechanism. Where that work addresses the question of *why Bayes factors operate on the moderate deviation scale*, this paper addresses a logically distinct question: *why does any goodness-of-fit calibration under Bayes risk operate on the moderate deviation scale, regardless of whether a Bayes factor or likelihood-ratio representation is available?*

Our (ρ, κ) template applies to statistics that are not likelihood ratios, including Kolmogorov–Smirnov statistics, empirical-process functionals, and divergence-based tests, and does not require the alternative to be specified through a parametric model. The moderate deviation scaling emerges here as a structural consequence of risk balancing, not as a property of any particular testing paradigm; the MDP regime is

where the problem lives, regardless of the statistic used to interrogate it. A companion development (Polson et al., 2026) extends these ideas to the sequential setting, showing that a Fubini decomposition of Bayes risk under log-loss identifies the likelihood ratio as the canonical e-value and that the moderate-deviation scale governs boundary selection for anytime-valid inference.

Under standard regularity, classical GOF statistics, namely Kolmogorov–Smirnov, likelihood-ratio, Pearson χ^2 , and entropy-deficit criteria, share the same Sanov rate function $\text{KL}(G\|F_0)$ (Sanov, 1957; Hoeffding, 1965). Good’s (1955) weight-of-evidence framework and Jaynes’s (1957) maximum-entropy formulation recover this rate function from complementary starting points. These equivalence results explain why Lemma 2.8 produces the same MDP scaling across seemingly disparate GOF statistics: once ρ and κ are identified, the Bayes-risk mechanism is indifferent to the choice of statistic.

The Bayesian testing literature has long recognised that posterior model probabilities depend on the tail behaviour of the marginal likelihood (Dawid, 2011). Carota et al. (1996) develop a complementary perspective, constructing diagnostic measures for model criticism that quantify the sensitivity of posterior inferences to local perturbations of the assumed model; their framework highlights precisely the kind of prior-to-likelihood geometry that, in our setting, is captured by the interplay of ρ and κ . The present paper makes this dependence explicit and quantitative: the marginal likelihood’s tail rate is governed by ρ , while the prior’s local geometry contributes κ . This two-parameter reduction complements Dawid’s (1992) prequential perspective, in which the cumulative predictive log-likelihood serves as the fundamental measure of model adequacy. In our framework, the prequential criterion’s growth rate under the alternative determines κ , closing the circle between risk-based and prediction-based approaches.

8.3 Implications for Scientific and Regulatory Practice

The results have practical consequences for the calibration of statistical tests in settings where sample sizes vary across studies or accumulate sequentially.

First, the Bayes-risk perspective implies that rejection thresholds should evolve with sample size. A fixed significance level α is optimal only in the degenerate case where no prior mass accumulates near the null; once the prior is absolutely continuous near \mathcal{F}_0 , the MDP threshold $t_n^* \propto \sqrt{\log n}$ strictly dominates any constant threshold in terms of aggregate decision risk. Our results suggest that fixed significance thresholds may not optimally balance aggregate decision risk when information accumulates with sample size.

Second, the (ρ, κ) template provides a principled basis for sample-size-dependent calibration in adaptive trial designs. In group-sequential or information-monitoring frameworks, the spending function that allocates Type I error across interim analyses can be informed by the MDP scaling: the optimal error rate at information level n is $\alpha_n \asymp n^{-\kappa/2}$, with κ reflecting the effective dimensionality of the alternative space under consideration.

Third, the connection to model selection is suggestive. When GOF testing is embedded in model comparison among K families, a heuristic application of the (ρ, κ) template with the Schwarz-type Occam factor (Schwarz, 1978) suggests a penalty of the form $(d/2) \log n + \log K$, paralleling the Bayesian information criterion; a rigorous derivation requires verifying the regularity conditions of Theorem 2.6 in the model-selection context and is left to future work. Similarly, for simultaneous GOF tests across $J = J(n)$

hypotheses, a Bonferroni-type adjustment suggests the threshold inflates to $t_n \approx \sqrt{a^* \log(nJ)}$, though the formal justification requires extending the risk decomposition to the multiple-testing setting.

Fourth, in high-dimensional screening where the number of parameters grows with n , the effective exponent κ becomes dimension-dependent. The template accommodates this by treating $\kappa = \kappa(d)$ as a function of the growing parameter dimension, though explicit rates require case-by-case analysis of the prior concentration behaviour.

As a concrete illustration, Table 1 translates the (ρ, κ) pairs into explicit threshold constants: for a KS test at $n = 10,000$, the Bayes-optimal significance level is approximately $\alpha_n \approx n^{-1} \approx 10^{-4}$, far below the conventional 0.05 yet far above the exponentially small levels associated with a large-deviation threshold. For a χ^2 test with $k = 10$ categories, the optimal exponent $a^* = 9$ yields $\alpha_n \approx n^{-4.5}$, reflecting the higher effective dimensionality of the alternative space. These values provide ready-to-use calibration guidance for practitioners willing to adopt sample-size-dependent thresholds. These remarks are normative within the Bayes-risk objective and do not preclude fixed-level frequentist calibration for alternative inferential goals.

8.4 Directions for Further Research

Several extensions merit investigation. First, the present analysis assumes independent observations; extending the (ρ, κ) template to dependent data, including mixing processes, time series, and spatial models, requires replacing the Brownian-bridge tail with the appropriate weak-convergence limit and verifying that the prior mass condition adapts to the effective sample size.

Second, high-dimensional settings in which the parameter dimension d grows with n present both opportunities and challenges. When $\kappa = \kappa(d)$ depends on a diverging dimension, the MDP threshold may transition from $\sqrt{\log n}$ to a different scaling; characterising this transition and its implications for Bayes-risk optimality is an open problem.

Third, sequential and online testing frameworks, where data arrive continuously and decisions must be made in real time, call for an MDP analogue of the sequential probability ratio test. The connection between MDP-optimal calibration and e-value or safe testing (Datta et al., 2026; Polson et al., 2026) suggests a natural bridge, though the formal development of the GOF-specific sequential theory remains to be carried out.

Finally, extending the (ρ, κ) template to minimax or Γ -minimax formulations, where the prior is replaced by a least-favourable distribution over a class of priors, remains an open question, as does the behaviour of the MDP scaling under alternative loss functions or infinite-dimensional nuisance parameters.

The moderate deviation boundary thus serves as a bridge between classical large-deviation theory and contemporary Bayesian risk calibration. Within the class of priors and statistics satisfying the sub-Gaussian tail and polynomial local mass conditions, the (ρ, κ) template reveals that the MDP scale is the unique locus at which the geometry of evidence and the structure of prior uncertainty are in balance.

References

R. R. Bahadur. Stochastic comparison of tests. *Annals of Mathematical Statistics*, 31:276–295, 1960.

R. R. Bahadur and R. R. Rao. On deviations of the sample mean. *Annals of Mathematical Statistics*, 31: 1015–1027, 1960.

J. O. Berger. *Statistical Decision Theory and Bayesian Analysis*. Springer, New York, 2nd edition, 1985.

J. O. Berger and T. Sellke. Testing a point null hypothesis: The irreconcilability of P values and evidence. *Journal of the American Statistical Association*, 82:112–122, 1987.

H. Chernoff. A measure of asymptotic efficiency for tests of a hypothesis based on the sum of observations. *Annals of Mathematical Statistics*, 23:493–507, 1952.

C. Carota, G. Parmigiani, and N. G. Polson. Diagnostic measures for model criticism. *Journal of the American Statistical Association*, 91:753–762, 1996.

T. M. Cover and J. A. Thomas. *Elements of Information Theory*. Wiley, Hoboken, NJ, 2nd edition, 2006.

Jyotishka Datta, Nicholas G. Polson, Vadim Sokolov, and Daniel Zantedeschi. A new look at Bayesian testing. *arXiv preprint arXiv:2602.11132*, 2026.

A. P. Dawid. Prequential analysis, stochastic complexity and Bayesian inference. In J. M. Bernardo, J. O. Berger, A. P. Dawid, and A. F. M. Smith, editors, *Bayesian Statistics 4*, pages 109–125. Oxford University Press, Oxford, 1992.

A. P. Dawid. Posterior model probabilities. In P. S. Bandyopadhyay and M. Forster, editors, *Philosophy of Statistics*, pages 607–630. Elsevier, New York, 2011.

A. P. Dawid and M. Musio. Bayesian model selection based on proper scoring rules. *Bayesian Analysis*, 10: 479–499, 2015.

A. Dembo and O. Zeitouni. *Large Deviations Techniques and Applications*. Springer, New York, 2nd edition, 1998.

I. J. Good. The likelihood ratio test for Markoff chains. *Biometrika*, 42:531–533, 1955.

J. Hájek and Z. Šidák. *Theory of Rank Tests*. Academic Press, New York, 1967.

W. Hoeffding. Asymptotically optimal tests for multinomial distributions. *Annals of Mathematical Statistics*, 36:369–401, 1965.

E. T. Jaynes. Information theory and statistical mechanics. *Physical Review*, 106:620–630, 1957.

H. Jeffreys. *Theory of Probability*. Oxford University Press, 3rd edition, 1961.

R. E. Kass and A. E. Raftery. Bayes factors. *Journal of the American Statistical Association*, 90:773–795, 1995.

J. Kiefer and J. Wolfowitz. Consistency of the maximum likelihood estimator in the presence of infinitely many incidental parameters. *Annals of Mathematical Statistics*, 27:887–906, 1956.

L. Le Cam. *Asymptotic Methods in Statistical Decision Theory*. Springer, New York, 1986.

D. V. Lindley. A statistical paradox. *Biometrika*, 44:187–192, 1957.

N. G. Polson, V. Sokolov, and D. Zantedeschi. Bayes, e-values, and testing. *arXiv preprint arXiv:2602.04146*, 2026.

H. Rubin and J. Sethuraman. Bayes risk efficiency. *Sankhyā*, 27:347–356, 1965a.

H. Rubin and J. Sethuraman. Probabilities of moderate deviations. *Sankhyā*, 27:325–346, 1965b.

I. N. Sanov. On the probability of large deviations of random variables. *Matematicheskii Sbornik*, 42:11–44, 1957. In Russian; English translation in *Selected Translations in Mathematical Statistics and Probability*, 1:213–244, 1961.

G. Schwarz. Estimating the dimension of a model. *Annals of Statistics*, 6:461–464, 1978.

G. L. Sievers. On the probability of large deviations and exact slopes. *Annals of Mathematical Statistics*, 40: 1908–1921, 1969.

D. J. Spiegelhalter. An omnibus test for normality for small samples. *Biometrika*, 67:493–496, 1980.

D. J. Spiegelhalter and A. F. M. Smith. Bayes factors for linear and log-linear models with vague prior information. *Journal of the Royal Statistical Society, Series B*, 42:213–232, 1980.

S. T. Tokdar and R. E. Kass. Importance sampling: A review. *Wiley Interdisciplinary Reviews: Computational Statistics*, 2:54–60, 2010.

V. A. Uthoff. An optimum test property of two well-known statistics. *Journal of the American Statistical Association*, 65:1597–1600, 1970.

A. W. van der Vaart and J. A. Wellner. *Weak Convergence and Empirical Processes*. Springer, New York, 1996.

S. L. Zabell. R. A. Fisher and the fiducial argument. *Statistical Science*, 7:369–387, 1992.

A Proofs of Technical Results

A.1 Proof of Theorem 3.6 (KS Bayes-optimal threshold)

We provide a careful proof that makes explicit where the $\sqrt{\log n}$ threshold and exponent enter.

Proof. Consider tests $\delta_{n,t}(x^n) = \mathbf{1}\{\sqrt{n}S_n > t\}$ with threshold $t = t_n$. Write the Bayes risk (3) as

$$B_n(t) = \pi_0 L_0 \underbrace{\mathbb{P}_0(\sqrt{n}S_n > t)}_{\alpha_n(t)} + \pi_1 L_1 \underbrace{\mathbb{E}_{\Pi_1} [\mathbb{P}_F(\sqrt{n}S_n \leq t)]}_{\bar{\beta}_n(t)}. \quad (41)$$

Since $\pi_0 L_0$ and $\pi_1 L_1$ are positive constants, they do not affect the optimiser a^* ; we absorb them into the \asymp notation below.

Step 1: Type I tail on the Kolmogorov scale. By the Brownian-bridge supremum asymptotics, for $t = \sqrt{a \log n}$,

$$\alpha_n(\sqrt{a \log n}) \asymp n^{-2a}. \quad (42)$$

Step 2: Uniform Type II bound outside the critical KS ball. Fix $F \in \mathcal{F}_1$ with $\varepsilon = d_{KS}(F, F_0) > 0$. Since $S_n \geq \varepsilon - \sup_x |F_n(x) - F(x)|$, whenever $\varepsilon \geq 2t/\sqrt{n}$, the DKW inequality gives

$$\mathbb{P}_F(\sqrt{n}S_n \leq t) \leq 2e^{-n\varepsilon^2/2}. \quad (43)$$

Step 3: Prior integration and the critical neighbourhood. Define $\rho_n = t/\sqrt{n}$ and split by KS-distance:

$$\bar{\beta}_n(t) = \int_{d_{KS} \leq 2\rho_n} \mathbb{P}_F(\sqrt{n}S_n \leq t) \Pi_1(\mathrm{d}F) + \int_{d_{KS} > 2\rho_n} \mathbb{P}_F(\sqrt{n}S_n \leq t) \Pi_1(\mathrm{d}F).$$

The first integral is bounded by $\Pi_1(d_{KS} \leq 2\rho_n) \asymp \rho_n^\kappa$ (Assumption 3.1). The second integral is $o(\rho_n^\kappa)$ by (43). For $t = \sqrt{a \log n}$:

$$\bar{\beta}_n(\sqrt{a \log n}) \asymp (a \log n/n)^{\kappa/2}. \quad (44)$$

Step 4: Optimisation and the polylogarithmic refinement. The refined Type II analysis (Rubin–Sethuraman) replaces the crude bound with a Laplace-method evaluation over a thin KS shell, producing an additional t factor: $\bar{\beta}_n(t) \asymp t(t/\sqrt{n})^\kappa = t^{\kappa+1}/n^{\kappa/2}$. With $t = \sqrt{a \log n}$, the risk becomes $B_n(\sqrt{a \log n}) \asymp n^{-2a} + a^{(\kappa+1)/2} (\log n)^{(\kappa+1)/2} n^{-\kappa/2}$. At leading order in n , setting $n^{-2a} = n^{-\kappa/2}$ gives $a^* = \kappa/4$. The factor $a^{(\kappa+1)/2}$ contributes only at polylogarithmic order:

$$t_n^* = \sqrt{\frac{\kappa}{4} \log n} + O(\sqrt{\log \log n}). \quad (45)$$

□

A.2 Proof of Proposition 4.2

Proof. **Step 1: Dual inequality.** Fix $t \geq 0$ and any $G \ll F_0$. Using the tilt decomposition,

$$\text{KL}(G\|F_0) = \text{KL}(G\|F_t) + t \int \phi \, dG - \Lambda(t).$$

Since $\text{KL}(G\|F_t) \geq 0$ and $\int \phi \, dG \geq 0$ for $G \in H$ with $t \geq 0$: $\text{KL}(G\|F_0) \geq -\Lambda(t)$. Taking inf over $G \in H$ and sup over $t \geq 0$ gives the lower bound.

Step 2: Achievability. If there exists $t^* > 0$ with $\Lambda'(t^*) = 0$, take $G^* = F_{t^*}$. Since $\int \phi \, dF_{t^*} = \Lambda'(t^*) = 0$, we have $G^* \in H$ and $\text{KL}(F_{t^*}\|F_0) = 0 + t^* \cdot 0 - \Lambda(t^*) = -\Lambda(t^*)$. If no interior optimiser exists, a sequence $t_k \uparrow$ with $-\Lambda(t_k) \uparrow \sup_{t \geq 0} \{-\Lambda(t)\}$ and $F_{t_k} \in H$ eventually yields the reverse inequality by lower semicontinuity. □

B Triangulation of Evidence Measures

This appendix establishes that four classical measures of evidence, namely Bayes factors, likelihood ratios, entropy deficits, and large-deviation rates, coincide locally through KL curvature, providing the geometric foundation for the moderate-deviation calibration developed in the main text.

B.1 Multinomial Setup

Let X_1, \dots, X_n be i.i.d. categorical with k categories. Write the null hypothesis probability vector as $\theta_0 = (\theta_{01}, \dots, \theta_{0k})$ with $\theta_{0j} > 0$ and $\sum_j \theta_{0j} = 1$. The empirical distribution is $\hat{p} = (n_1/n, \dots, n_k/n)$, where $n_j = \#\{i : X_i = j\}$. The Kullback–Leibler divergence from θ_0 to \hat{p} is

$$D(\hat{p} \parallel \theta_0) = \sum_{j=1}^k \hat{p}_j \log \frac{\hat{p}_j}{\theta_{0j}}. \quad (46)$$

B.2 Good → Bayes Factor → KL + log n

Good (1955) evaluated the weight of evidence as the logarithm of the Bayes factor. A Laplace approximation to the marginal likelihood under a Dirichlet prior on the alternative simplex yields

$$W = n D(\hat{p} \parallel \theta_0) + \frac{k-1}{2} \log n + O(1). \quad (47)$$

The first term is the leading exponential evidence; the second is the Occam–complexity correction from integrating over the $(k-1)$ -dimensional simplex.

B.3 Hoeffding → Sanov → KL Rate

Hoeffding (1965) showed that the probability of a type class under the null decays at the Sanov rate:

$$\frac{1}{n} \log \mathbb{P}_{\theta_0}(\hat{p} \in A) \rightarrow - \inf_{Q \in A} D(Q \parallel \theta_0). \quad (48)$$

For the multinomial, the likelihood ratio statistic is $\Lambda_n = 2n D(\hat{p} \parallel \theta_0)$ exactly, so the exponential rate of the likelihood ratio is governed by the same KL divergence.

B.4 Jaynes → Entropy Deficit

Jaynes (1957) characterised the null θ_0 as the maximum-entropy distribution subject to the relevant moment constraints. The entropy deficit from the null to the empirical distribution satisfies the exact identity

$$H^* - H(\hat{p}) = D(\hat{p} \parallel \theta_0) + \sum_j (\hat{p}_j - \theta_{0j}) \log \theta_{0j}, \quad (49)$$

where $H^* = -\sum_j \theta_{0j} \log \theta_{0j}$ is the null entropy and $H(\hat{p}) = -\sum_j \hat{p}_j \log \hat{p}_j$. For a uniform null ($\theta_{0j} = 1/k$), the cross-entropy correction vanishes since $\sum_j (\hat{p}_j - \theta_{0j}) = 0$, giving $\Delta H = D(\hat{p} \parallel \theta_0)$ exactly. In the general

case, $2n \Delta H = 2n D(\hat{p} \parallel \theta_0) + 2n \sum_j (\hat{p}_j - \theta_{0j}) \log \theta_{0j}$, where the correction term is $O_{\mathbb{P}}(\sqrt{n})$.

B.5 Quadratic Closure $\rightarrow \chi^2$

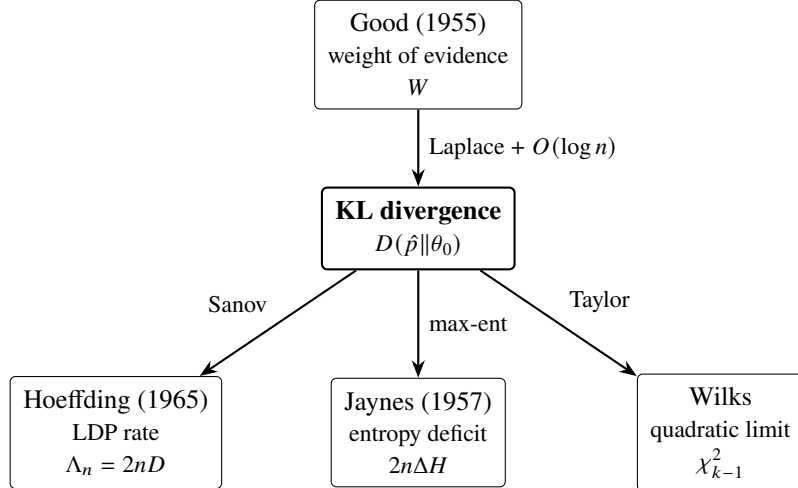
Expanding the KL divergence to second order around θ_0 gives the Wilks approximation:

$$2n D(\hat{p} \parallel \theta_0) = \sum_{j=1}^k \frac{(n_j - n\theta_{0j})^2}{n\theta_{0j}} + o_{\mathbb{P}}(1) \rightarrow \chi_{k-1}^2. \quad (50)$$

Combining the three leading-order representations yields the quadratic closure identity. For the uniform null ($\theta_{0j} = 1/k$), where $\Delta H = D(\hat{p} \parallel \theta_0)$ exactly:

$$\boxed{\Lambda_n = 2n \Delta H = 2n D(\hat{p} \parallel \theta_0) \sim \chi_{k-1}^2.} \quad (51)$$

For non-uniform θ_0 , the entropy deficit includes a cross-entropy correction: $2n \Delta H = \Lambda_n + 2n \sum_j (\hat{p}_j - \theta_{0j}) \log \theta_{0j}$. Good's weight of evidence differs by the Occam factor: $2W = \Lambda_n + (k-1) \log n + O(1)$.



All roads meet at KL curvature.

Figure 7: Triangulation of evidence measures. Good's weight of evidence connects to the KL core through a Laplace approximation with an $O(\log n)$ Occam correction; the remaining three frameworks converge exactly through Kullback–Leibler curvature.

B.6 Bridge to the Main Text

This triangulation reveals that Bayes factors, likelihood ratios, entropy deficits, and large-deviation rates are not alternative measures of evidence but different coordinate representations of a single geometric object: the KL curvature at the null. The moderate-deviation calibration developed in the main text therefore operates within a unified geometric framework linking Bayesian, frequentist, and information-theoretic representations.

C Computational Methods

C.1 Monte Carlo Estimation of Bayes Risk

For GOF settings where analytic calibration is unavailable, Bayes risk can be estimated by Monte Carlo. Draw $F^{(1)}, \dots, F^{(M)} \sim \Pi_1$ and, for each m , simulate $X^{(m)} \sim (F^{(m)})^{\otimes n}$ and compute $T_n^{(m)}$. The Type II term at threshold t is estimated by $\widehat{\beta}_n(t) = M^{-1} \sum_{m=1}^M \mathbf{1}\{T_n^{(m)} \leq t\}$. The Type I term may be estimated by simulation under F_0 or via a known tail approximation; importance-sampling methods (Tokdar and Kass, 2010) can reduce variance substantially. Finally, minimise $\widehat{B}_n(t) = \pi_0 L_0 \widehat{\alpha}_n(t) + \pi_1 L_1 \widehat{\beta}_n(t)$ over a grid of t . This Monte Carlo illustration is solely a sanity check; all reported thresholds in Section 7 are deterministic evaluations of the analytic risk expression.

C.2 Estimating the Local Prior Exponent

If Π_1 is specified implicitly, probe Π_1 near the null by Monte Carlo: estimate $p_j = \Pi_1(d(F, F_0) \leq \varepsilon_j)$ for shrinking radii ε_j and regress $\log p_j \approx \kappa \log \varepsilon_j + \text{const.}$

C.3 Asymptotic Plug-in Approximation

In the MDP regime with null tail $\mathbb{P}(T_\infty > t) \asymp e^{-2\rho t^2}$, a convenient approximation is

$$t_n^* \approx \sqrt{\frac{\hat{\kappa}}{4\rho} \log n}, \quad (52)$$

where $\hat{\kappa}$ is the estimated local prior exponent and ρ is the tail-rate parameter (e.g., $\rho = 1$ for the KS Brownian-bridge tail).

D Extended Numerical Tables

This appendix supplements the numerical verification of Section 7 with detailed threshold tables for each main theorem.

D.1 KS Thresholds (Theorem 3.6)

With $\rho = 1$ (Brownian-bridge tail $\sim 2e^{-2t^2}$) and varying κ , Table 3 compares the Bayes-optimal MDP threshold $t_n^* = \sqrt{\kappa \log n / 4}$ against the constant fixed- α critical value $K^{-1}(0.95) \approx 1.358$.

For $\kappa \geq 5$ the MDP threshold already exceeds the fixed- α value at $n = 100$; as n grows, the gap widens steadily. The Bayes risk $B_n^* \asymp (\log n / n)^{\kappa/2}$ decays polynomially.

D.2 Multinomial χ^2 Thresholds (Theorem 5.8)

With $\rho = 1/4$ and $\kappa = k - 1$ (Dirichlet prior), Table 4 compares the MDP critical value $\chi_n^{2*} = (k - 1) \log n$ against the conventional $\chi_{k-1}^2(0.95)$ quantile.

Table 3: KS Bayes-optimal thresholds ($\rho = 1$). The MDP threshold grows with n ; the fixed- α threshold does not.

κ	n	t_n^* (MDP)	t (fixed α)	α_n^*	B_n^*
1	100	1.073	1.358	1.0×10^{-1}	2.1×10^{-1}
	1 000	1.314	1.358	3.2×10^{-2}	8.3×10^{-2}
	10 000	1.517	1.358	1.0×10^{-2}	3.0×10^{-2}
	10^6	1.858	1.358	1.0×10^{-3}	3.7×10^{-3}
2	100	1.517	1.358	1.0×10^{-2}	4.6×10^{-2}
	1 000	1.858	1.358	1.0×10^{-3}	6.9×10^{-3}
	10 000	2.146	1.358	1.0×10^{-4}	9.2×10^{-4}
	10^6	2.628	1.358	1.0×10^{-6}	1.4×10^{-5}
5	100	2.399	1.358	1.0×10^{-5}	4.6×10^{-4}
	1 000	2.938	1.358	3.2×10^{-8}	4.0×10^{-6}
	10 000	3.393	1.358	1.0×10^{-10}	2.6×10^{-8}
	10^6	4.156	1.358	1.0×10^{-15}	7.1×10^{-13}
10	100	3.393	1.358	1.0×10^{-10}	2.1×10^{-7}
	1 000	4.156	1.358	1.0×10^{-15}	1.6×10^{-11}
	10 000	4.799	1.358	1.0×10^{-20}	6.6×10^{-16}
	10^6	5.877	1.358	1.0×10^{-30}	5.0×10^{-25}

Table 4: Multinomial χ^2 Bayes-optimal thresholds ($\rho = 1/4$).

k	κ	n	χ_n^{2*} (MDP)	$\chi_{\kappa}^2(0.95)$	α_n^*
3	2	100	9.2	5.99	1.0×10^{-2}
	2	1 000	13.8	5.99	1.0×10^{-3}
	2	10 000	18.4	5.99	1.0×10^{-4}
4	3	100	13.8	7.81	1.0×10^{-3}
	3	1 000	20.7	7.81	3.2×10^{-5}
	3	10 000	27.6	7.81	1.0×10^{-6}
10	9	100	41.4	16.92	1.0×10^{-9}
	9	1 000	62.2	16.92	3.2×10^{-14}
	9	10 000	82.9	16.92	1.0×10^{-18}

For $k = 10$ categories at $n = 10,000$, the Bayes-optimal critical value of 82.9 is nearly 5× the fixed- α value of 16.92. This reflects the multiplicity cost of servicing a $(k-1)$ -dimensional alternative space under Bayes risk.

D.3 Fisher Rejection Radii (Theorem 6.2)

With $\rho = 1/4$ and $\kappa = \lambda + d$, Table 5 shows the Fisher-distance rejection radius $r_n^* = \sqrt{(\lambda + d) \log n/n}$ for several configurations of prior exponent λ and parameter dimension d .

Table 5: Fisher-distance rejection radii ($\rho = 1/4$, $\kappa = \lambda + d$).

λ	d	κ	$n = 100$	$n = 1,000$	$n = 10,000$	$n = 100,000$
1	1	2	0.3035	0.1175	0.0429	0.0152
1	2	3	0.3717	0.1440	0.0526	0.0186
2	3	5	0.4799	0.1858	0.0679	0.0240
1	5	6	0.5257	0.2036	0.0743	0.0263

The radii shrink as $\sqrt{\log n/n}$, strictly slower than the $n^{-1/2}$ rate of CLT-scale procedures but strictly faster than the $O(1)$ resolution of LDP-scale tests.